Optimization of Simultaneous Co-located Transmission to meet both Regulatory Limits and Performance Requirements

Dissertation submitted to

Visvesvaraya National Institute of Technology, Nagpur

in partial fulfillment of the requirements for the award of the degree

Master of Technology

in

Communication System Engineering

by

Ayushi S. Jaiswal (MT23CMN006)

Under the guidance of

Dr. Ankit A. Bhurane

Assistant Professor, Department of ECE, VNIT

Department of Electronics and Communication Engineering

Visvesvaraya National Institute of Technology

Nagpur 440 010 (India)

June 2025

Optimization of Simultaneous Co-located Transmission to meet both Regulatory Limits and Performance Requirements

Dissertation submitted to

Visvesvaraya National Institute of Technology, Nagpur

in partial fulfillment of the requirements for the award of the degree

Master of Technology

in

Communication System Engineering

by

Ayushi S. Jaiswal (MT23CMN006)

Under the guidance of

Dr. Ankit A. Bhurane

Assistant Professor, Department of ECE, VNIT

Department of Electronics and Communication Engineering

Visvesvaraya National Institute of Technology

Nagpur 440 010 (India)

June 2025

© Visvesvaraya National Institute of Technology (VNIT) 2025

Department of Electronics and Communication
Visvesvaraya National Institute of Technology, Nagpur

Declaration

I, **Ayushi S. Jaiswal**, hereby declare that this dissertation titled "**Optimization of Simultaneous Co-Located Transmission to meet both Regulatory Limits and Performance Requirements**" is carried out by me in the Department of Electronics and Communication of Visvesvaraya National Institute of Technology, Nagpur. The work is original and has not been submitted earlier whole or in part for the award of any degree /diploma at this or any other Institution / University.

Ayushi S. Jaiswal
Date:

Certificate

This to certify that the dissertation titled "**Optimization of Simultaneous Co-Located Transmission to meet both Regulatory Limits and Performance Requirements**" is submitted by **Ayushi S. Jaiswal** in partial fulfillment of the requirements for the award of the degree of **Master of Technology** in **Communication System Engineering**, VNIT Nagpur. The work is comprehensive, complete and fit for final evaluation.

Dr. Ankit A. Bhurane
Assistant Professor,
Department of Electronics and Communication,
VNIT, Nagpur

Prof. Ashwin G. Kothari
Professor and Head,
Department of Electronics and Communication,
VNIT, Nagpur

NON-PLAGIARISM CERTIFICATE

VERIFIED AND APPROVED

2/6/2025

(ANKIT A. BHURANE)

3% Overall Similarity

The combined total of all matches, including overlapping sources, for each database.

Filtered from the Report

- Bibliography
- Quoted Text

Exclusions

- 6 Excluded Matches

Match Groups

32 Not Cited or Quoted 3%
Matches with neither in-text citation nor quotation marks

0 Missing Quotations 0%
Matches that are still very similar to source material

0 Missing Citation 0%
Matches that have quotation marks, but no in-text citation

0 Cited and Quoted 0%
Matches with in-text citation present, but no quotation marks

Top Sources

2% Internet sources
3% Publications
0% Submitted works (Student Papers)

Integrity Flags

0 Integrity Flags for Review

No suspicious text manipulations found.

Our system's algorithms look deeply at a document for any inconsistencies that would set it apart from a normal submission. If we notice something strange, we flag it for you to review.

A Flag is not necessarily an indicator of a problem. However, we'd recommend you focus your attention there for further review.

ACKNOWLEDGEMENT

I would like to express my sincere gratitude to all those who supported me throughout the course of this thesis.

First and foremost, I am deeply thankful to my supervisor, Dr. Ankit A. Bhurane, for his invaluable guidance, continuous support, and encouragement throughout the research and writing process. His expertise and insightful feedback played a crucial role in shaping the direction and quality of this work.

I extend my heartfelt thanks to Prof. Ashwin Kothari, Head of the Department, for providing a supportive academic environment.

Further, I am grateful to my internship managers at NXP Semiconductors, Pune; Mr. Vishal Veeragandham and Mr. Aveek Bhattacharya, for their understanding, flexibility, and encouragement, which allowed me to balance professional responsibilities with academic commitments.

I would also like to extend my sincere gratitude to the Silicon Validation Co-ex team at NXP, including the team lead, Mr. Mahesh Nahar, and team members Mr. Akash Kambale, Mr. Mangesh Perala, and Ms. Surabhi Sinha, for their guidance, clear explanations, and unwavering support throughout the project. Their contributions significantly deepened my understanding and played a crucial role in the advancement of this project.

I am deeply indebted to my parents and my sister for their unwavering motivation and constant support, which sustained me throughout this endeavor.

I am also thankful to my friends for their continual support and encouragement at various stages of my academic journey.

Finally, I offer my regards to all those who contributed to the successful completion of this thesis both directly and indirectly.

ABSTRACT

The integration of multiple wireless technologies into a single system-on-chip (SoC) has greatly improved device connectivity and interoperability. However, this progress also brings new challenges, especially when multiple radios operate at the same time and in close proximity, both physically and spectrally. The compact nature of these systems leads to tightly packed antennas and greater interaction among RF front-end components. Because these components are inherently nonlinear, signal coupling can occur, resulting in different types of distortion, particularly intermodulation products and harmonics.

Among these, third-order intermodulation distortion (IMD3) is especially important in the 2.4 GHz ISM band, which is heavily used by technologies like Wireless Local Area Networks (WLAN) and Bluetooth. IMD3 degrades in-band communication quality and causes spectral regrowth, which can interfere with nearby licensed frequency bands and raise regulatory concerns. As the need for smooth multi-radio coexistence increases, it is important to understand how IMD3 is generated and how it can be mitigated to ensure reliable wireless communication.

This thesis investigates the sources and behavior of IMD3 in scenarios where WLAN and Bluetooth operate together. It reviews mitigation techniques, like TX arbitration and power backoff methods. A Python-based simulation framework is developed to model IMD3 and evaluate the effectiveness of these techniques under different system conditions. The simulation results support the theoretical analysis and show that the proposed methods help reduce distortion and improve coexistence.

The findings of this study contribute to the development of more reliable and interference-resistant wireless systems. They provide both theoretical insights and practical tools for addressing distortion caused by nonlinearities in integrated multi-radio platforms.

Keywords: WLAN, Bluetooth, Third – Order Intermodulation Distortions, Coexistence, TX-TX Mode, Power Amplifier, Nonlinearity

TABLE OF CONTENTS

Abstract i

List of Figures v

List of Tables viii

List of Abbreviations ix

List of Publications xi

Chapter 1 Introduction 1

1.1 Overview 1

1.2 Introduction to Wireless Technologies 2

1.2.1 Wireless Local Area Network (WLAN) 2

1.2.2 Bluetooth Technology 3

1.3 TX-TX Interference: The Coexistence Issue 5

1.3.1 Causes of Signal Coupling in Concurrent Transmissions 6

1.3.2 Unwanted Spectral Components: Harmonics and Intermodulation Products 7

1.4 Problem Statement 8

1.5 Thesis Organization 8

Chapter 2 Analysis of IMD3 in Wireless Communication Circuits 9

2.1 Introduction to Third-Order Intermodulation Distortions 9

2.2 Impact of IMD3 on Other Applications 11

2.3 Hardware Test Setup for IMD3 Measurements in RF Systems 13

2.4 Radio Characteristics Affecting the IMD3 Performance 15

2.4.1 Transmit Power of both the Radios 15

2.4.2 Isolation Between the Two Transmitting Antennas 15

2.4.3 Frequency Separation between the Transmitting Channels 15

2.4.4 WLAN Modulation Type 16

2.4.5 Bluetooth Modulation Type 16

2.5 Terminology Used in the IMD3 Analysis 17

Chapter 3 IMD3 Mitigation Techniques in RF and Wireless Systems 18

3.1 Transmission Arbitration in Coexisting Networks 19

3.2 Power Backoff Method for Interference Mitigation 20

3.3 Integrated Implementation of the Two Techniques 21

3.4 Implementation of Mitigation Techniques in Hardware Architectures 24

3.5 Optimization of PA Parameters 25

Chapter 4 Implementation of IMD3 Mitigation Techniques using Python-Based Automation 27

4.1 Tool Algorithm 28

4.1.1 Stage 1: Input to the Automation Tool 29

4.1.2 Stage 2: Post Processing of the Raw Data 31
4.1.3 Stage 3: Organization of Data and TX Arbitration Sheet Generation 33
4.1.4 Stage 4: Deriving WLAN and Bluetooth Feedback Powers 37
4.1.5 Stage 5: Evaluating the Register Values 39
4.1.6 Stage 6: Storing the Register Values in the Output File 43

Chapter 5 Results and Conclusion 45
5.1 Results of the Python Automation Tool 45
5.1.1 Stage 1: Raw Input Data for Automation Processing 46
5.1.2 Stage 2: Output After Data Post-Processing 47
5.1.3 Stage 3: Output after TX Arbitration and Data Organization 48
5.1.4 Output After Applying Power Backoff Technique 49
5.1.5 Stage 5 & 6: Output of Prepared Register Configurations 50
5.2 Conclusion 52
5.3 Future Scope 52

References 54

LIST OF FIGURES

Figure No.	Description	Page No.
1.1	WLAN Channel Distribution in the 2.4 GHz ISM Band	3
1.2	Channel Distribution for BTC and BLE in 2.4 GHz ISM Band	4
1.3	TX-to-TX Interference when both Radios Operate in TX Mode Simultaneously	5
1.4	RF Transmit Chain with One Antenna	6
2.1	Generation of Intermodulation Products when Signals Pass Through a Nonlinear System	10
2.2	Formation of IMD3 Components when both Radios are in TX Mode	11
2.3	IMD3 Products Falling on Adjacent Frequency Components Within and Outside the ISM Band Causing Interference	12
2.4	Conducted Test Setup used for Measuring IMD3 Levels on a Hardware Chipset (DUT)	13
2.5	Contour Plots for IMD3 Variations with respect to WLAN and Bluetooth Transmit Powers	14
3.1	Proposed TX-to-TX Power Backoff Technique with the Aggressor WLAN TX Signal at the Victim Bluetooth TX Output	21
3.2	Flowchart Showing Integrated Implementation of TX Arbitration and Power Backoff Technique	22
3.3	IMD3 Performance as a function of WLAN and Bluetooth TX Powers for Different Antenna Isolations	23

3.4	Flowchart Showing Implementation of Mitigation Techniques on Hardware using Firmware	25
4.1	Complete Algorithm for Python Based Implementation of IMD3 Mitigation Techniques	28
4.2	Flowchart Representing Derivation of Additional Fields from the Raw Input Data	33
4.3	Division of Complete Bluetooth TX Power Range into Eight Bins	34
4.4	Flowchart Showing Segregation of Processed Data w.r.t Measurement Parameters	36
4.5	Block Diagram to Show Generation of Final TX Arbitration Sheet	37
4.6	Logic for Identification of Feedback Power by the Algorithm	38
4.7	Flowchart Showing Process of Determining Feedback Powers for Lower Priority Radio	39
4.8	Evaluation of Hardware Register Values for TX Arbitration Technique	41
4.9	Assignment of Evaluated Register Values to Register Addresses as per Hardware Definition for TX Arbitration Technique	42
4.10	Evaluation of Hardware Register Values for Power Backoff Technique	43
5.1	Output Files Generated by the Python Based Implementation Tool	45

5.2	WLAN Victim IMD3 Measurement Input Data for The Automation Tool	46
5.3	Bluetooth Victim IMD3 Measurement Input Data for the Automation Tool	47
5.4	WLAN Processed Data with Updated Columns	47
5.5	Bluetooth Processed Data with Updated Columns	48
5.6	Organized WLAN Victim Data w.r.t Measurement Parameters and Power Bins	48
5.7	Final TX Arbitration Sheet	49
5.8	Feedback Powers - WLAN Low Priority Scenario	50
5.9	Feedback Powers - Bluetooth Low Priority Scenario	50
5.10	Final Automation Output 1 - TX Arbitration Hardware Register Addresses and Respective Values	51
5.11	Final Automation Output 2 - Hardware Register Addresses and Respective Values Representing Power Backoff Technique	51

LIST OF TABLES

Table No.	Description	Page No.
2.1	Different Intermodulation Products, their Contributing Components and Orders	10
4.1	Input Raw Data - Measured IMD3 levels for WLAN Victim with respect to Influencing Parameters	30
4.2	Input Raw Data - Measured IMD3 levels for Bluetooth Victim with respect to Influencing Parameters	30
4.3	Input Parameters given at Stage 2	32
4.4	Bluetooth Bins and their Respective Power Bin Representatives	35

LIST OF ABBREVIATIONS

WLAN	Wireless Local Area Network
ISM	Industrial, Scientific, and Medical
RF	Radio Frequency
SoC	System on Chip
DSSS	Direct Sequence Spread Spectrum
OFDM	Orthogonal Frequency Division Multiplexing
QAM	Quadrature Amplitude Modulation
SIG	Special Interest Group
BTC	Bluetooth Classic
BLE	Bluetooth Low Energy
BR	Basic Rate
EDR	Enhanced Data Rate
GFSK	Gaussian Frequency Shift Keying
DQPSK	Differential Quadrature Phase Shift Keying
DPSK	Differential Phase Shift Keying
DAC	Digital-to-Analog Converter
PA	Power Amplifier
IMD	Intermodulation Distortion
IMD3	Third-Order Intermodulation Distortion
FCC	Federal Communications Commission

DUT	Device Under Test
PAPR	Peak-to-Average Power Ratio
TX	Transmit

LIST OF PUBLICATIONS

1. Ayushi Jaiswal, Ankit Bhurane “Analysis of Intermodulation Distortion in Integrated RF Coexistence,” in *Emerging Technologies Shaping New Communication and Electronic Infrastructures*, E. Ogbodo, Ed., IGI Global Scientific Publishing, 2025.

Gmail Ayushi Jaiswal <ayushijaiswal2000@gmail.com>

Chapter Approved

1 message

IGI Global Scientific Publishing Book Submission System <booksubmissionsystemadmin@igi-global.com> Sat, May 3, 2025 at 11:58 AM
Reply-To: eugene.ogbodo@gmail.com
To: ayushijaiswal2000@gmail.com
Cc: eugene.ogbodo@gmail.com

eEditorial Discovery
Supporting Your Editorial Experience

Dear Ayushi Jaiswal,

NOTE: Your references must be in APA before your chapter can be published and I encourage you to try an increase the number of references to between 15 and 25

I am pleased to inform you that your chapter, "Analysis of Intermodulation Distortion in Integrated RF Coexistence," submitted to "Emerging Technologies Shaping New Communication and Electronic Infrastructures" has passed the editorial review phase. Next, your chapter will be submitted to IGI Global Scientific Publishing for a final check to ensure that all publication requirements have been met.

Should any of your chapter materials be missing or need to be corrected, you will be contacted by a member of the IGI Global Scientific Publishing development team to secure the necessary details prior to publication. If you need to upload any new or revised materials to finalize your submission, you may do so here: https://www.igi-global.com/submission/submit-chapter/?chapterid=11121608-663d-466d-bdbf-35f521593d87&s=4

No chapter will be accepted unless it strictly follows the manuscript guidelines, i.e., references and in-text citations formatted according to APA style guidelines, include all mandatory sections (Introduction, Background, Future Research Directions, Conclusion, References, Additional Reading, and Key Terms & Definitions), etc.

All manuscripts submitted for consideration to IGI Global Scientific Publishing must be professionally copy edited. IGI Global Scientific Publishing highly recommends eContent Pro's English language copy-editing services as part of the Standard Editorial Package. All past and present IGI Global Scientific Publishing authors and editors receive an exclusive 25% discount on these services. Click here to learn more.

Additionally, you may want to consider converting your manuscript to open access in order to increase the discoverability of your published work and accelerate its citation impact. This can be done at any time, even post-publication. Authors publishing under OA will have their work published under the CC BY 4.0 license which allows them to retain the copyright to their work with no commercial restrictions while making the research fully free and accessible to all. IGI Global Scientific Publishing offers a number of funding programs including IGI Global Scientific Publishing's OA Fee Waiver (Read and Publish) Initiative. To see if you are currently eligible for an open access Chapter Processing Charge (CPC) waiver and/or to learn more about how to benefit from the program, please contact openaccessadmin@igi-global.com for more information.

After the manuscript is arrived in production by the development editor, alterations beyond minor corrections (especially grammatical and punctuation changes) are not permitted. Changes that involve only matters of style will not be carried out by the typesetter, as we have introduced the IGI Global Scientific Publishing house style. Substantial changes in content (new results, corrected values) are not allowed. Revised proofs will not be sent to the author.

Should you have any questions regarding this email, please do not hesitate to contact me, Eugene Ogbodo, at eugene.ogbodo@gmail.com.

IGI Global Scientific Publishing
eEditorial Discovery

CHAPTER 1

INTRODUCTION

1.1 Overview

Wireless communication technologies have rapidly evolved over the past decade, enabling high-speed data transfer and seamless connectivity across various applications. Two prominent technologies that drive wireless communication are WLAN and Bluetooth [1] [2]. WLAN is governed by IEEE 802.11 standards. It provides high speed connectivity for internet access and local networking [3]. Bluetooth technology on the other hand is based on IEEE 802.15.1 standard. It is optimized for short range and low power communication and is commonly used for connecting personal devices [4].

WLAN operates across three distinct ISM frequency bands: 2.4 GHz, 5 GHz, and 6 GHz. In contrast, Bluetooth is confined to the 2.4 GHz ISM band [5]. When these technologies are deployed independently, they function efficiently within their designated frequency channels. However, simultaneous operation in close proximity, particularly within the shared 2.4 GHz band can result in mutual interference [6]. This interference gives rise to coexistence challenges and often leads to a noticeable degradation in overall system performance [7].

As modern devices increasingly require seamless connectivity across different protocols. The integration of multiple radios within a single system has largely increased. Therefore, addressing this issue of cross-technology interference is essential to maintain reliable performance of wireless devices and to ensure compliance with regulatory standards [8] [9].

The work done in this project focuses on the coexistence issues when WLAN and Bluetooth operate in a single SoC. It aims to examine the impact of interferences caused due to simultaneous operation of these technologies and propose methods of mitigating them. The study involves detailed analysis of mitigation techniques implemented in practical scenarios. The work also includes the development of a tool that facilitates the implementation of these

mitigation techniques on real-time measured data on a hardware chipset. Formulation of the tool is done using Python Programming language.

The following section provides a detailed overview of the two wireless technologies that are considered in this project.

1.2 Introduction to Wireless Technologies

This subsection provides a detailed overview of the two wireless technologies, WLAN and Bluetooth, that are considered in this project.

1.2.1 Wireless Local Area Network (WLAN)

WLAN is one of the most widely adopted and efficient wireless communication technologies in use today. Its specifications are governed by the IEEE 802.11 family of standards. It is further subdivided into several amendments, including 802.11 *a*, *b, g, n, ac, ax* and *be*. These sub-standards differ in several key aspects such as supported transmission channels, output power levels, bandwidth capabilities, and, most notably, their modulation techniques [3].

Standards like 802.11b, g, n, and ax support communication within the 2.4 GHz spectrum. Meanwhile, 802.11a, n, ac, and ax function in the 5 GHz band. The newer generations, such as 802.11ax (also referred to as Wi-Fi 6/6E) and 802.11be (Wi-Fi 7), extend their operation to the 6 GHz frequency range, offering enhanced performance and capacity.

The performance of these standards is also significantly influenced by the modulation techniques employed. For instance, 802.11b utilizes the Direct Sequence Spread Spectrum (DSSS) method, while 802.11a, g, n, ac, and ax rely on Orthogonal Frequency Division Multiplexing (OFDM). Wi-Fi 7 further advances this by supporting modulation schemes up to 4096-QAM, enabling higher data rates and improved spectral efficiency.

Additionally, WLAN channels operate with bandwidths of 20 MHz, 40 MHz, 80 MHz and 160 MHz, with Wi-Fi 7 expanding this to as much as 320 MHz. Figure 1.1 shows frequency

channel distribution in the 2.4 GHz ISM band for WLAN. Here the channels are divided within 2400 MHz to 2483.5 MHz. Each channel is 20 MHz wide and is spaced 5 MHz apart from adjacent channels. A total of 14 channels are defined, though not all are available in every region due to regulatory differences [10].

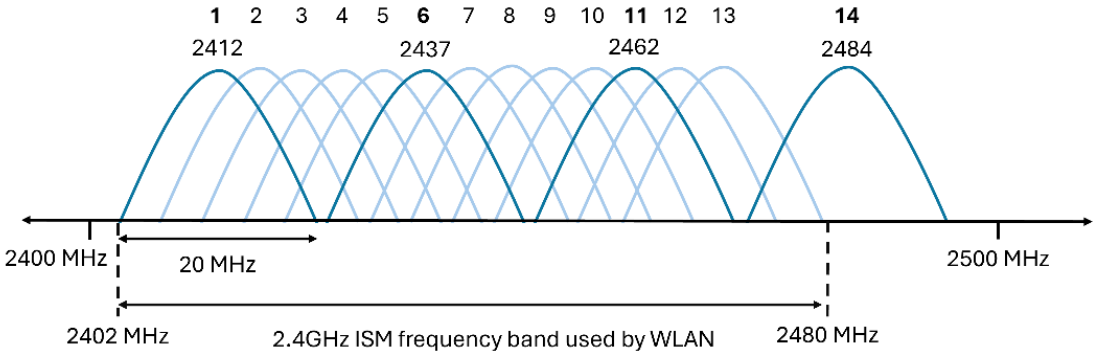

Figure 1.1: WLAN Channel Distribution in the 2.4 GHz ISM Band

Due to the limited spacing and overlapping bandwidths, most of the channels interfere with one another when used simultaneously. To reduce interference and maintain reliable performance, only three non-overlapping channels - channel 1, 6, and 11 are typically used in practical WLAN deployments. Channel 14 is uniquely used by Japan and is restricted to transmission of 802.11b at 11 Mbps.

1.2.2 Bluetooth Technology

Bluetooth technology is specified under the IEEE 802.15.1 standard and is governed by the Bluetooth Special Interest Group (SIG). It offers two major radio options: Bluetooth Classic (BTC) and Bluetooth Low Energy (BLE). Both variants operate within the 2.4 GHz unlicensed ISM frequency band, utilizing transmission channels ranging from 2402 MHz to 2480 MHz. The key distinction between the two radio types is in the channel bandwidth they use. BTC employs 1 MHz-wide channels, whereas BLE utilizes 2 MHz-wide channels [11].

The following Figure 1.2 illustrates the distribution of BTC and BLE channels across the 2.4 GHz band, highlighting their respective allocation strategies within the shared spectrum.

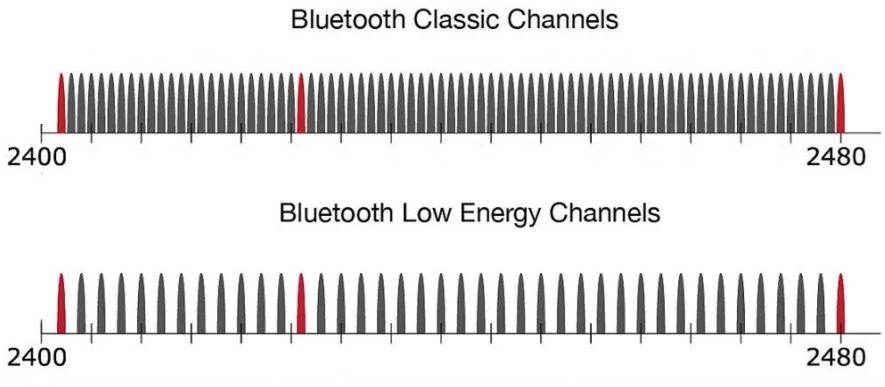

Figure 1.2: Channel Distribution for BTC and BLE in 2.4 GHz ISM Band

Further, BTC supports two data rate modes: the Basic Rate (BR), with a data rate of approximately 1 Mbps, and the Enhanced Data Rate (EDR), offering up to approximately 3 Mbps. The BR mode uses the Gaussian Frequency Shift Keying (GFSK) modulation, while EDR employs more complex schemes such as π/4-DQPSK and 8DPSK to achieve higher throughput. BLE, in contrast, uses GFSK modulation exclusively, which is optimized for low power and reduced complexity [12].

One another difference in the two radios is the supported topologies. BTC supports point-to-point device communication and is mainly used to enable wireless audio streaming. On the other hand, BLE supports multiple communication topologies, including point-to-point, broadcast and mesh. While initially known for its device communication capabilities, BLE is now also widely used as a device positioning technology. It can help one device in determine the presence, distance, and direction of another device.

Additionally, Bluetooth devices are also classified based on the maximum transmission power they can support. This limit directly affects the communication range. These classifications include:

1. Class 1: Up to 100 mW (approximately 100 meters range)

2. Class 2: Up to 2.5 mW (approximately 10 meters range)
3. Class 3: Up to 1 mW (approximately 1 meter range)

1.3 TX-TX Interference: The Coexistence Issue

The research undertaken in this project addresses the challenges associated with the concurrent transmission (TX-TX mode) of WLAN and Bluetooth technologies in the 2.4 GHz unlicensed ISM band. This subsection provides a concise overview of the coexistence scenarios, relevant to such simultaneous operation.

To enhance the performance and functionality of modern devices, WLAN and Bluetooth modules are often integrated onto the same SoC. This integration results in minimal physical separation between the two radio antennas. Since both technologies operate within the 2.4 GHz frequency band and are located in close physical proximity, the likelihood of signal coupling is significantly high. This poses considerable challenges in scenarios involving collocated transmissions [13].

The following Figure 1.3 presents a schematic representation of the SoC, where two radio antennas supporting WLAN and Bluetooth, respectively are positioned in close proximity. This configuration leads to coexistence challenges between the two wireless technologies when transmitted simultaneously [14].

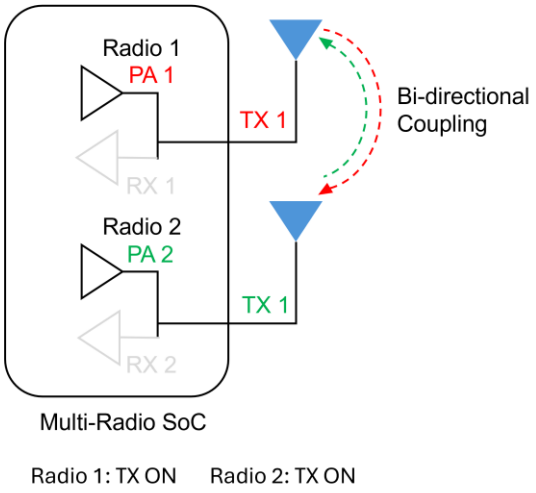

Figure 1.3: TX-to-TX Interference when both Radios Operate in TX Mode Simultaneously

1.3.1 Causes of Signal Coupling in Concurrent Transmissions

The coupling between the two transmitted signals is primarily attributed to the nonlinear behavior of one or more components within the RF transmit chain [15]. To enable wireless transmission within the RF spectrum, the RF transmit chain typically includes components such as digital-to-analog converters (DACs), mixers, filters, power amplifiers (PA), and antennas. Each of these components plays a vital role in processing and transmitting the desired signal. A basic RF transmit chain with a single transmitting antenna is illustrated in Figure 1.4.

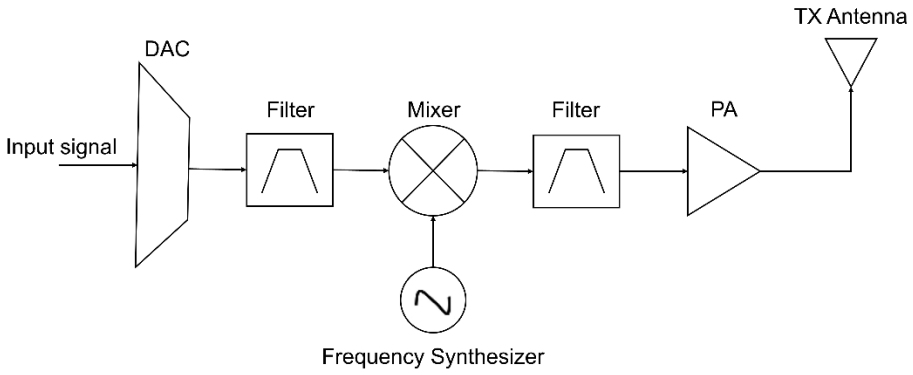

Figure 1.4: RF Transmit Chain with One Antenna

A similar RF chain is used for transmitting WLAN and Bluetooth signals. The component that majorly differentiates between the two transmit chains is the power amplifier. Since the Bluetooth signal is a constant envelope signal with only 1 MHz modulation bandwidth a single-cascode PA is generally employed. On the other hand, WLAN is an OFDM signal with up to 20 MHz modulation bandwidth, a double or higher cascode PA architectures are used. PA is the primary component exhibiting nonlinear behavior within the transmit chain of both the radios [16].

When WLAN and Bluetooth signals are transmitted simultaneously in the same frequency spectrum, the limited isolation between the radio antennas lets a portion of one transmitted signal to leak into the transmit chain of the other [14]. This leaked signal interacts with the desired radio signal at input of the other PA. This results in an additional coupled output due

to the PA nonlinearity. Consequently, the output of the PA contains not only the amplified intended signal but also the resultant coupled signal which causes interference.

The unwanted coupled signals are generated at the nearby frequencies of the actual channels. These components either appear at integer multiples of the actual transmit channel frequencies or at the sum or difference of the two frequencies. Two primary types of distortion signals that are typically generated are harmonic distortions and intermodulation distortions.

1.3.2 Unwanted Spectral Components: Harmonics and Intermodulation Products

Harmonics are frequency components that occur at integer multiples of a signal's fundamental frequency, which, in this context, corresponds to either of the two transmitting channel frequencies[15]. As the harmonic order increases, the magnitude of the components typically decreases, and their frequencies shift further away from the desired signal. Therefore, higher-order harmonics often fall outside the bandwidth of the amplifier or the passband of the filters. On the other hand, lower-order harmonics can be effectively suppressed using passband filters, due to high separation from the desired frequencies. Thus, higher-order harmonics are generally negligible due to their minimal potential for causing interference and lower order components can be readily suppressed through appropriate filtering techniques.

The major focus of this project is on the intermodulation distortions (IMD). IMD are unwanted signals generated when two or more different frequencies mix in a nonlinear system, producing additional frequency components at sum and difference of the original signals [15]. In the context of WLAN and Bluetooth coexistence, IMD product are primarily generated due to signal coupling at the PA. Higher order intermodulation products are of less concern as they are very far from the transmit channel frequencies. But the products that fall close to the desired frequencies are difficult to filter and they interfere with other applications resulting in regulatory failures. The concerns associated with IMD, along with mitigation techniques used for reducing their impact, are discussed in detail in the subsequent chapters.

1.4 Problem Statement

This project provides a comprehensive analysis and understanding of the interference issues arising from the coexistence of multiple wireless technologies, with a particular focus on WLAN and Bluetooth systems. The study primarily concentrates on third-order intermodulation distortions, which interfere with applications operating on adjacent frequency bands. Additionally, two mitigation techniques aimed at reducing the impact of these distortions are explored in the context of the identified problem.

1.5 Thesis Organization

This thesis is organized into five chapters, each providing a comprehensive discussion on interference issues arising in coexistence scenarios and the techniques employed to mitigate these unwanted signals.

The first chapter outlined the problem statement by summarizing WLAN-Bluetooth coexistence challenges. The second chapter focuses on third-order intermodulation distortions (IMD3), exploring their causes, impact on other applications, hardware-based measurements, and the key parameters influencing IMD3 performance. The third chapter presents two mitigation techniques studied during the course of this project. Chapter four describes the development and implementation of a tool designed for this study, highlighting its Python-based execution. The final chapter summarizes the work, presents the main results and conclusions, and discusses potential directions for future research. All references used in the course of this project are listed at the end of the thesis.

CHAPTER 2

ANALYSIS OF IMD3 IN WIRELESS COMMUNICATION CIRCUITS

Intermodulation distortions are unwanted interfering signals that arise when multiple radios operate concurrently within the same frequency bands. Among these, third-order intermodulation distortions are particularly critical due to their proximity to the fundamental frequencies, making them more likely to interfere with desired signals. This chapter presents a comprehensive overview of IMD3, discusses its implications on coexisting applications, describes the hardware setup employed for its measurement, and outlines the key parameters influencing IMD3 performance.

2.1 Introduction to Third-Order Intermodulation Distortions

Intermodulation distortion products are generated when two signals pass through a nonlinear device. In wireless communication systems, this typically occurs when WLAN and Bluetooth signals pass through the PA present in either of the RF transmit chains. These distortion components appear at frequencies corresponding to the sum and difference of the two transmitted channel frequencies[15]. For instance, if the WLAN signal is transmitted at frequency f_1 and the Bluetooth signal at frequency f_2, the resulting IMD products will appear at frequencies $f_1 \pm f_2$. Figure 2.1 shows a simple representation of this example.

The frequencies f_1 and f_2 may also couple with their respective harmonic components, leading to the generation of higher-order IMD products at $2f_1 \pm f_2$, $f_1 \pm 2f_2$, $3f_1 \pm f_2$ or $f_1 \pm 3f_2$ (etc.) frequencies. The order of each IMD product is determined by sum of the coefficients of the two interacting frequencies. Table 2.1 illustrates a few examples of IMD products resulting from the coupling of different frequency components.

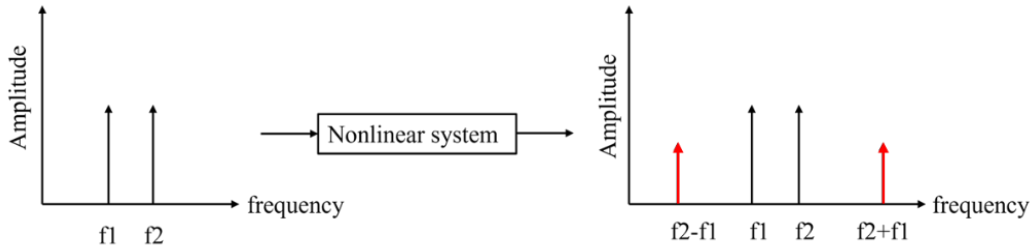

Figure 2.1: Generation of Intermodulation Products when Signals Pass Through a Nonlinear System

The components generated at frequencies corresponding to the sum of the fundamental frequencies are very far from the actual desired channels, therefore the interference caused by them is negligible. Ex. $2f_1 + f_2$, $f_1 + 2f_2$, $3f_1 + f_2$

Table 2.1: Different Intermodulation Products, their Contributing Components and Orders

Sr. No.	First frequency component	Second frequency component	Frequency of resultant IMD product	Order of the IMD product
1.	f_1 (fundamental frequency)	f_2 (fundamental frequency)	$f_1 \pm f_2$	2nd Order
2.	f_1 (fundamental frequency)	$2f_2$ (second harmonic)	$f_1 \pm 2f_2$	3rd Order
3.	$2f_1$ (second harmonic)	f_2 (fundamental frequency)	$2f_1 \pm f_2$	3rd Order
4.	$2f_1$ (second harmonic)	$2f_2$ (second harmonic)	$2f_1 \pm 2f_2$	4th Order
5.	$2f_1$ (second harmonic)	$3f_2$ (third harmonic)	$2f_1 \pm 3f_2$	5th Order

Among all the IMD products generated, the third-order intermodulation distortion (IMD3) components have the most adverse impact on the desired channel frequencies [17]. Other order IMD products generally appear farther from the desired channels and can be effectively filtered out using bandpass filters. However, IMD3 products typically fall near the operating bandwidth, making them difficult to suppress. Thus, they are the primary source of interference in the coexistence of multiple radios.

Figure 2.2 illustrates the formation of IMD3, when both WLAN and Bluetooth radios, placed on the same SoC, transmit simultaneously. As a result of this concurrent transmission, two third-order distortion components are generated on the respective PA side. The component appearing on the higher side of the frequency spectrum is referred to as IMD3H, while the one on the lower side is denoted as IMD3L.

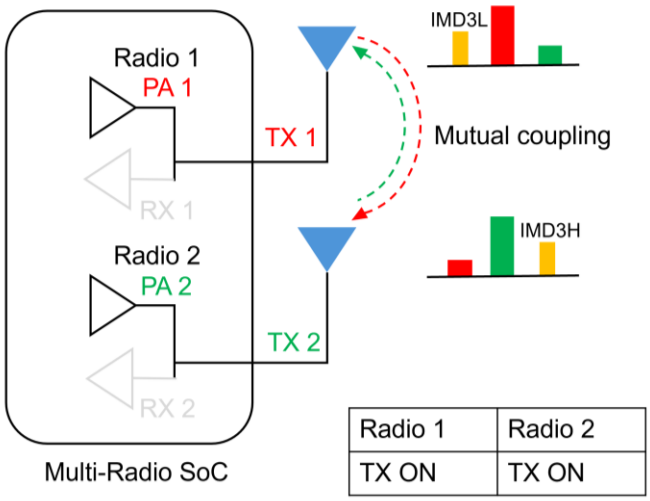

Figure 2.2: Formation of IMD3 Components when both Radios are in TX Mode

2.2 Impact of IMD3 on Other Applications

Both WLAN and Bluetooth operate within the 2.4 GHz unlicensed ISM band, with channel frequencies ranging from 2400 MHz to 2485 MHz. However, IMD3 products resulting from the coupling of these signals may appear either within this ISM band or in adjacent licensed frequency bands. If these IMD3 components fall within the ISM band, they can interfere with other applications already operating on those frequencies. More critically, if they occur in

neighboring licensed bands, they may lead to regulatory violations and potential penalties. Overall, the presence of IMD3 not only degrades system efficiency but also breaks compliance with communication standards [18]. Figure 2.3 shows a simple representation of how IMD3 products can fall outside the ISM bands.

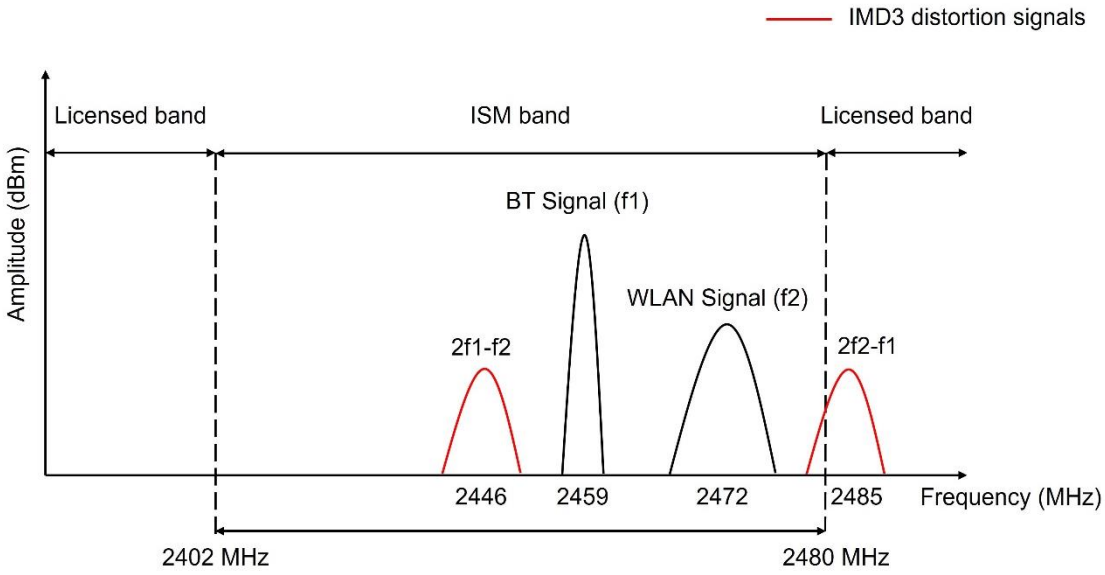

Figure 2.3: IMD3 Products Falling on Adjacent Frequency Components Within and Outside the ISM Band Causing Interference

The level of interference caused by IMD3 signals largely depends on their amplitude. If the strength of these unwanted distortion components remains within specified regulatory limits, the resulting interference is minimal. To ensure compliance, several international regulatory bodies have established maximum allowable limits for IMD3 signal levels. Devices that exceed these limits are deemed non-compliant and unsuitable for operation. One such regulatory authority is the Federal Communications Commission (FCC). Its specifications are referenced throughout this project to guide design decisions and evaluations. The specification defined by the FCC for IMD3 is –41.2 dBm/MHz[1], and this threshold must not be exceeded

[1] The –41.2 dBm/MHz limit is an FCC Part 15 spurious emission requirement for applications in unlicensed band, applied to all out-of-band emissions measured with a 1 MHz bandwidth.

[19]. Any IMD3 level within this range is considered acceptable and does not raise concerns regarding interference.

2.3 Hardware Test Setup for IMD3 Measurements in RF Systems

IMD3 levels can be measured using a simple hardware setup. To evaluate IMD3 performance across various configurations of WLAN and Bluetooth radios, empirical measurements were carried out on multi-radio chipsets. This subsection describes the hardware components used in the measurement setup and highlights their key characteristics. Figure 2.4 illustrates the conducted test setup employed for measuring IMD3 levels across different chipsets. While real-world scenarios involve radiated signals, the conducted setup was used for this project due to its controlled environment and repeatability. It is important to note that the difference in IMD3 levels between conducted and radiated setups is typically negligible.

In this setup, an attenuator, a coupler, and a spectrum analyzer are used. The attenuator is used to provide external isolation between the two transmitting antennas. The coupler is placed between the two antennas to direct a portion of the attenuated signal from one radio into the path of the other, thereby enabling controlled signal coupling. The spectrum analyzer is used to observe and analyze the resulting signals. It displays the output, typically showing three distinct components: the WLAN signal, the Bluetooth signal, and the resulting IMD3 distortion products.

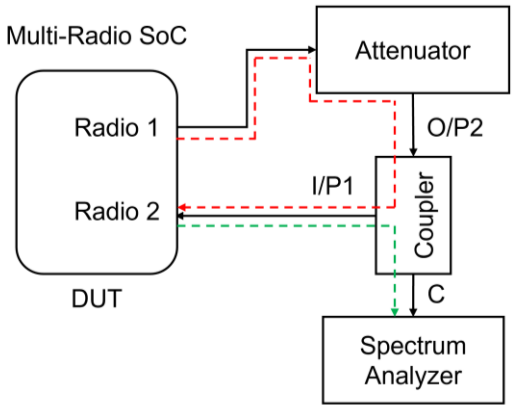

Figure 2.4: Conducted Test Setup used for Measuring IMD3 Levels on a Hardware Chipset (DUT)

The magnitude of IMD3 is highly dependent on the transmit power levels of the two radios. To examine this relationship, an analysis is usually conducted across different combinations of WLAN and Bluetooth transmit powers. Therefore, IMD3 behavior can be visualized in a three-dimensional space. Figure 2.5 presents a contour plot based on sample IMD3 measurements, where one axis represents the WLAN transmit power, the second axis corresponds to the Bluetooth transmit power, and different contours indicates the magnitude of the resulting IMD3 levels.

Figure 2.5 (a) illustrates the contour plot of IMD3 measurements observed at the WLAN PA side, while Figure 2.5 (b) depicts the IMD3 levels generated at the Bluetooth PA side.

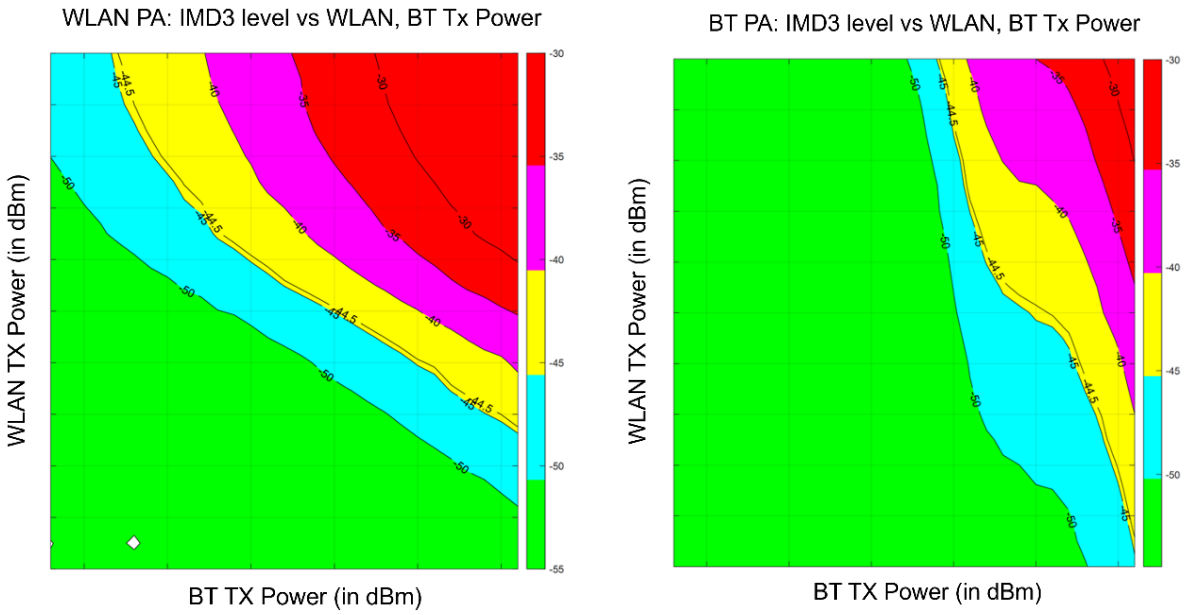
WLAN PA: IMD3 level vs WLAN, BT Tx Power
WLAN TX Power (in dBm)
BT TX Power (in dBm)
BT PA: IMD3 level vs WLAN, BT Tx Power
WLAN TX Power (in dBm)
BT TX Power (in dBm)

(a) (b)

Figure 2.5: Contour Plots for IMD3 Variations with respect to WLAN and Bluetooth Transmit Powers

2.4 Radio Characteristics Affecting the IMD3 Performance

The magnitude and position of the IMD3 signal generated as a result of coupling of WLAN and Bluetooth transmissions are significantly influenced by various characteristics of the two signals. This subsection outlines some of the key parameters that affect IMD3 behavior.

2.4.1 Transmit Power of both the Radios

The amplitude of the IMD3 signal is directly controlled by the transmit power levels of both WLAN and Bluetooth. Since IMD3 is a result of the convolution of the two radio signals, higher transmit powers from both radios lead to stronger distortion components. When both radios operate at their maximum power levels, the resulting IMD3 signal becomes significantly strong and poses a high risk of interference with other applications. Conversely, reducing the transmit power of either radio leads to a noticeable reduction in IMD3 signal strength.

2.4.2 Isolation Between the Two Transmitting Antennas

Since both radios operate within the same frequency range, antenna isolation plays a critical role in IMD3 performance. Low isolation between collocated antennas significantly increases the likelihood of signal coupling, which in turn leads to stronger and more adverse IMD3 signals. On the other hand, maintaining adequate isolation between the two antennas helps mitigate signal coupling, thereby reducing the strength of the IMD3 components. It is important to note, however, that the degree of antenna isolation is often determined by the specific application or use case that the chipset is designed to support.

2.4.3 Frequency Separation between the Transmitting Channels

Apart from antenna isolation, less frequency separation between the transmitting channels for WLAN and Bluetooth also increases the chances of coupling of the two signals. The

overlapping between the spectral components of the transmitted signals is significantly increased. This results in higher IMD3 amplitudes. Therefore, increasing the frequency separation can effectively improve IMD3 performance.

2.4.4 WLAN Modulation Type

Each WLAN standard employs distinct modulation and transmission techniques, which significantly influence the resulting IMD3 signal strength. For example, IEEE 802.11b uses DSSS, a relatively simple and narrowband modulation scheme that typically produces lower IMD3 levels. In contrast, more advanced standards such as IEEE 802.11n utilize OFDM, which, due to its higher peak-to-average power ratio (PAPR) and wider bandwidth, tends to generate stronger IMD3 components. This variation in IMD3 behavior is primarily attributed to differences in modulation complexity, signal bandwidth, and the number of simultaneous subcarriers or spatial streams, which increase the likelihood of nonlinear distortion and frequency overlap [10].

2.4.5 Bluetooth Modulation Type

Another factor influencing IMD3 signal strength is the data rate of the transmitted Bluetooth signal [20]. Bluetooth BR, which operates at a lower data rate of 1 Mbps using GFSK, generally produces lower IMD3 levels compared to Bluetooth EDR, which employs more complex modulation schemes such as π/4-DQPSK and 8DPSK at higher data rates (2–3 Mbps). Conversely, BLE, despite its low power operation, may contribute more to IMD3 due to its relatively wider signal bandwidth and use of frequency hopping. Overall, IMD3 performance is influenced by the modulation scheme, bandwidth, and data rate of the transmitted Bluetooth signal [11] [12].

In addition to the above-mentioned parameters, the transmission priority of the radios also affect IMD3 performance. This refers to which radio gets to transmit first when both radios raise requests simultaneously. The priority is usually based on the application each radio supports. In systems with multiple radios, assigning priority helps reduce interference. In

WLAN and Bluetooth coexistence, either radio can be given higher priority depending on the system's requirements.

2.5 Terminology Used in the IMD3 Analysis

Two key terms frequently used in IMD3 analysis are aggressor and victim. In simultaneous, collocated transmissions, one radio is designated as the aggressor, while the other is referred to as the victim. Among the two coexisting radios, the victim is the radio of interest, the one intended for the target application. The aggressor, on the other hand, is the unintended transmitter that operates in the shared frequency band. Its presence generate IMD3 components which degrades the overall system performance. Both these terms are used throughout the following chapters.

In case when Bluetooth and WLAN transmit simultaneously either of the radio can act as a victim or aggressor. It is the aggressor’s attenuated power that reach the victim PA, where the two signals couple resulting in IMD3 generation. To gain a complete understanding of IMD3 behavior, the measurements and the analysis is done with each radio alternately considered as the victim. Among the two IMD3 components generated, the one that appears closer to the victim radio’s channel frequency typically causes more interference. Therefore, this component is considered in the further analysis.

CHAPTER 3
IMD3 MITIGATION TECHNIQUES IN RF AND WIRELESS SYSTEMS

IMD3 is an inherent byproduct of nonlinearities present in the RF transmit chain. In practical RF systems, it is nearly impossible to avoid some level of nonlinearity, particularly because components such as power amplifiers, are intentionally operated in nonlinear regions to maximize power efficiency. While linear operation can minimize distortion, it often comes at the cost of reduced efficiency. As a result, the trade-off between linearity and efficiency makes the presence of IMD3 a persistent challenge in real-world RF transmitter designs. As a result, mitigation techniques are employed to reduce the strength of these distortion signals and minimize their interference with other systems [21]. This chapter presents two IMD3 mitigation techniques that were reviewed and analyzed during the course of this project.

To gain a comprehensive understanding of IMD3 behavior on a chipset, measurements were conducted across various test cases covering the full range of WLAN and Bluetooth transmit power levels. These test cases are primarily defined based on critical parameters known to significantly influence the IMD3 performance. The scenarios examined in this project include IMD3 measurements under varying frequency separations, different levels of antenna isolation, WLAN modulation schemes (802.11b and 802.11n), and all supported Bluetooth data rates.

The IMD3 response varies significantly with different combinations of influencing parameters. Therefore, the mitigation techniques are designed to effectively minimize interference caused by IMD3 under each specific scenario.

3.1 Transmission Arbitration in Coexisting Networks

The TX arbitration technique is based on a simple yet effective principle to suppress the IMD3 emissions. According to this technique when a higher-priority radio initiates transmission, the lower-priority radio should not be granted access in the shared frequency band. In cases where both collocated radios request transmission simultaneously, only the higher-priority radio is permitted, and the lower-priority request is denied. Furthermore, if the lower-priority radio is already transmitting and a higher-priority request comes in, the ongoing transmission from the lower-priority radio is aborted.

To implement this technique, IMD3 performance is evaluated over the entire range of WLAN and Bluetooth transmit power levels. Based on these measurements, arbitration decisions are derived by assessing the IMD3 amplitude for each possible power combination. If the measured IMD3 signal exceeds the FCC-specified threshold of –41.2 dBm/MHz, that specific transmit power combination is classified as unsuitable for simultaneous operation. Conversely, if the IMD3 level remains within the permissible limit, concurrent transmission of both radios at the corresponding power levels is considered acceptable.

These arbitration decisions are made for each WLAN and Bluetooth transmit power combination across all relevant parameter configurations. To streamline the representation of these decisions, the allowed cases can be represented by 1 and the prohibited cases by 0. Consequently, a complete analysis in terms of 1 and 0 is done to execute the arbitration decisions. The analysis file is made for all combinations of influencing parameters separately, like different frequency separations, WLAN modulations, Bluetooth data rates and various physical isolations in between the two transmitting antennas.

Although this technique appears easy to implement, it is not the most efficient way of reducing IMD3 distortion signals. Removing a radio from the transmitting frequency range will not generate IMD3 distortions but the concept of coexistence itself will be violated. The efficiency and scope of application of the device will greatly decline. Also, the channel for the lower priority radio that will be arbitrated will thus remain unused, affecting the overall system throughput. This technique is still applied in some practical SoCs where advanced mitigation techniques are not feasible due to hardware limitations or footprint constraints.

3.2 Power Backoff Method for Interference Mitigation

The second mitigation technique explored in this project is the power backoff strategy. This approach is based on the arbitration decisions discussed in the preceding section. In cases where simultaneous transmission of WLAN and Bluetooth is not allowed due to excessive IMD3 levels, this technique still allows the lower-priority radio to transmit at a reduced power level. This implies that the higher priority radio can continue to transmit at its requested power and the lower priority radio will be granted access with reduced transmit power as compared to what it actually requested [22].

Since the IMD3 signal amplitude is a result of the nonlinear interaction (convolution) of the two radio signals, reducing the transmit power of either radio leads to a corresponding reduction in the IMD3 amplitude. This forms the basis for defining the Power backoff technique. Although this technique does not completely eliminate IMD3, it effectively attenuates the distortion to remain within regulatory limits, thereby maintaining coexistence without compromising system functionality.

Figure 3.1 illustrates the impact of reducing the transmit power of one of the coexisting radios to effectively lower the overall IMD3 signal amplitude. In this example, the WLAN signal, transmitted at 20 dBm, acts as the aggressor and interferes with the Bluetooth signal, also transmitted at 20 dBm. The IMD3 generated due to Bluetooth PA is shown in the Figure. In the first scenario (represented by solid lines), both radios transmit at their requested power levels, leading to a significant IMD3 component at the higher frequency. In the second scenario (represented by dashed line), the WLAN transmit power is reduced by 5 dBm. As a result, the IMD3 amplitude has noticeably decreased.

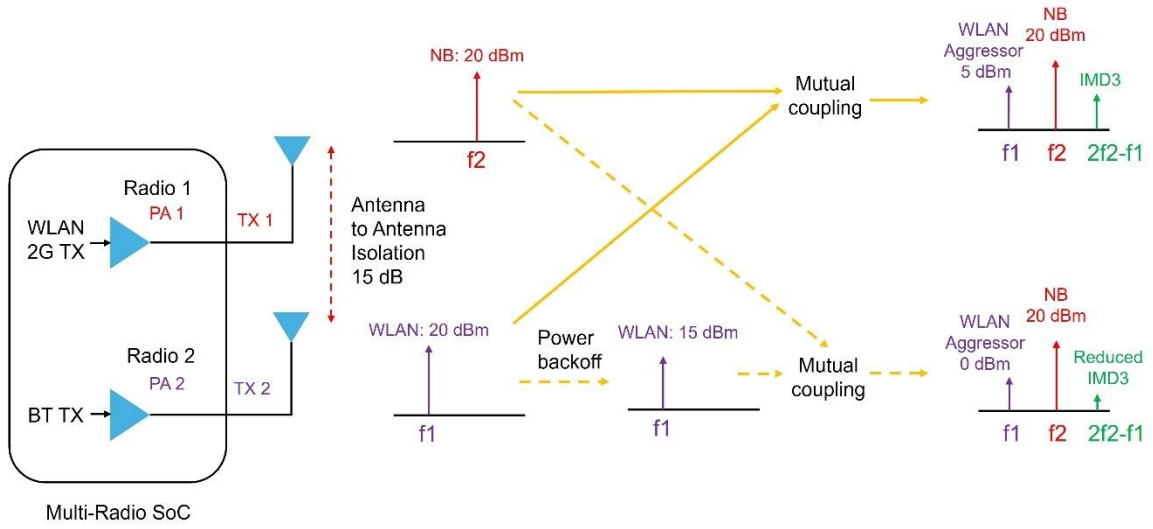

Figure 3.1: Proposed TX-to-TX Power Backoff Technique with the Aggressor WLAN TX Signal at the Victim Bluetooth TX Output

It is important to note that the aggressor signal (WLAN) reaches the victim radio (Bluetooth) after passing the cross radio path[2]; hence, the effective interference is determined by subtracting the antenna isolation from the actual WLAN transmit power.

3.3 Integrated Implementation of the Two Techniques

The two approaches, TX arbitration and power backoff, can be implemented collectively to reduce the interference caused due to IMD3 emissions. These techniques are implemented for the complete set of IMD3 measured data over different critical parameters. The first step after collecting the IMD3 measurement data is to make the arbitration decisions in terms of 1 and 0. Based on these decisions and assigned radio priorities, the feedback power for the lower priority radio is evaluated. This involves identifying the maximum allowed power that a lower

[2] In the hardware measurement setup, the cross-radio path is emulated using an attenuator that provides a constant level of isolation between the two co-located antennas.

priority radio can transmit simultaneously with the higher priority radio without violating the regulatory limits. The lower priority radio is then given grant to transmit at the lowered power level.

Figure 3.2 presents a detailed flowchart outlining the integrated implementation of the two proposed IMD3 mitigation techniques. In this scenario, both radios are assumed to be integrated on the same SoC, with minimal isolation between them, and operating within the same frequency range.

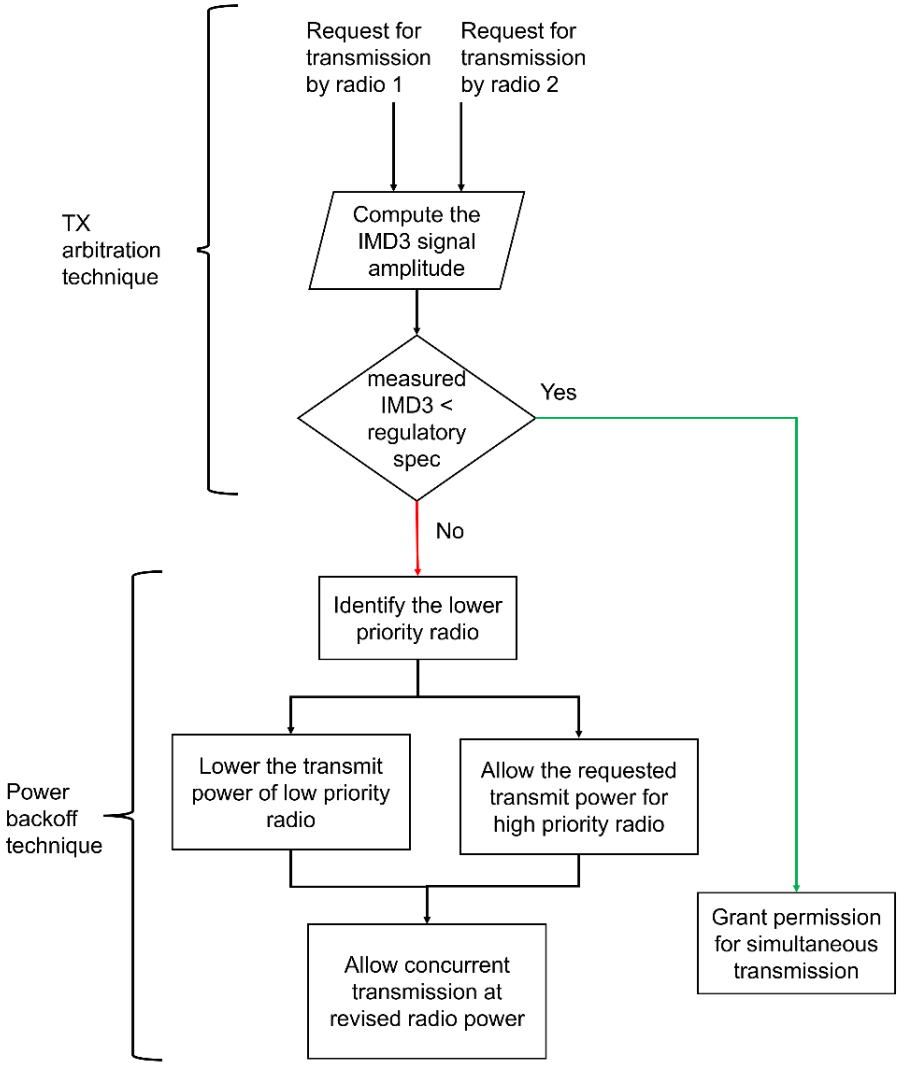
Request for transmission by radio 1
Request for transmission by radio 2
TX arbitration technique
Compute the IMD3 signal amplitude
measured IMD3 < regulatory spec
Yes
No
Identify the lower priority radio
Power backoff technique
Lower the transmit power of low priority radio
Allow the requested transmit power for high priority radio
Allow concurrent transmission at revised radio power
Grant permission for simultaneous transmission

Figure 3.2: Flowchart Showing Integrated Implementation of TX Arbitration and Power Backoff Technique

Since either coexisting radio can be in lower priority, the feedback power must be evaluated for both the radios. Therefore, for a fixed transmit power of the higher-priority radio, the feedback powers are calculated based on the measured IMD3 levels. This relationship can be illustrated using a plot with WLAN and Bluetooth transmit powers on the two axes.

Figure 3.3 shows the maximum allowed transmit powers, with WLAN power on the y-axis and Bluetooth power on the x-axis. The plot is bidirectional and can be interpreted from either axis. Different curves represent different level of isolation maintained between the two transmitting antennas. Each line represents the maximum transmit power permitted for simultaneous operation of the corresponding radio, without exceeding regulatory limits.

Consider the red curve representing 20 dB isolation, IMD3 measurements in Figure 3.3. The maximum allowed WLAN power, for 2.5 dBm Bluetooth power, is 12 dBm. If either of the two powers increase it will lead to IMD3 failures of the FCC specification. Therefore 12 dBm is the maximum allowed power that WLAN can transmit with 2.5 dBm Bluetooth power simultaneously and vice versa.

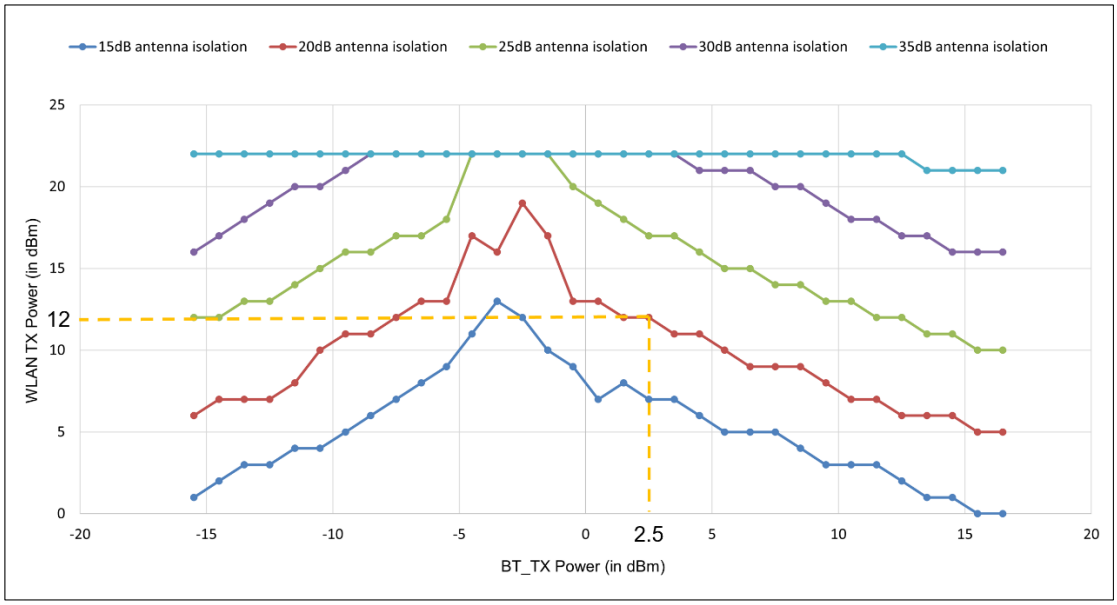

Figure 3.3: IMD3 Performance as a function of WLAN and Bluetooth TX Powers for Different Antenna Isolations

Since IMD3 measurements and the corresponding arbitration decisions are obtained for each combination of WLAN and Bluetooth transmit power levels, the area below each line represent all power combinations that are allowed for simultaneous transmission in the coexistence scenario. In contrast, the area above the lines indicates prohibited power combinations that may lead to regulatory failures.

In conclusion, the combined application of TX arbitration and power backoff enables effective coexistence between the two radios. Through detailed IMD3 measurements and arbitration analysis, a feedback power value is determined for the lower-priority radio at each transmit power level of the higher-priority radio. This coordinated approach allows both radios to transmit concurrently without violating emission standards, thereby preserving compliance and maintaining system performance.

3.4 Implementation of Mitigation Techniques in Hardware Architectures

Implementation of the two proposed techniques on the IMD3 measurement data gives two sets of results: one consisting of arbitration decisions represented in terms of 1 or 0, and the other comprising feedback power values corresponding to each transmit power level of the higher-priority radio. Since SoC platforms do not have built-in mechanisms to perform this analysis, all computations are carried out externally. However, for the system to operate in compliance with regulatory requirements, these results must be integrated into the chipset.

To achieve this, the arbitration decisions and feedback power values are encoded into hexadecimal format and programmed into the hardware. The chipset includes predefined register addresses reserved for these functions. Thus, the complete analysis is translated into register values and transferred to the hardware via firmware.

Figure 3.4 depicts the data flow, showing how the two techniques are applied and subsequently implemented on a SoC to ensure compliance with regulatory requirements.

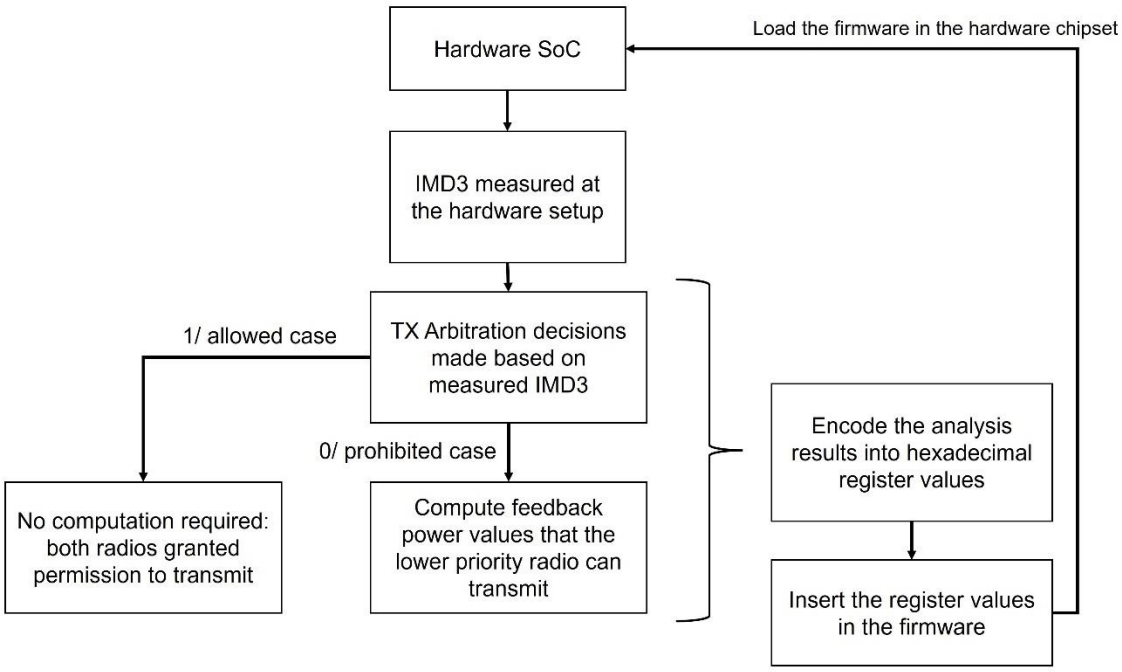
Hardware SoC
Load the firmware in the hardware chipset
IMD3 measured at the hardware setup
TX Arbitration decisions made based on measured IMD3
1/ allowed case
0/ prohibited case
No computation required: both radios granted permission to transmit
Compute feedback power values that the lower priority radio can transmit
Encode the analysis results into hexadecimal register values
Insert the register values in the firmware

Figure 3.4: Flowchart Showing Implementation of Mitigation Techniques on Hardware using Firmware

3.5 Optimization of PA Parameters

In addition to the IMD3 mitigation techniques, achieving maximum throughput in a multi-radio chipset also involves characterizing the PA parameters in two distinct modes:

- Efficiency-Based Mode: This mode is used when there is no simultaneous transmission from multiple radios. In such cases, the PA is allowed to operate in a way that prioritizes reducing the overall current consumption of the SoC, thereby improving power efficiency.
- IMD3-Optimized Mode: This mode is used during concurrent transmission scenarios. Here, the PA is configured so that the IMD3 distortions are minimized, ensuring better coexistence performance and regulatory compliance.

These PA characteristics are stored in configuration tables, which are programmed into the SoC. Based on different operational scenario, the SoC dynamically switches between the two tables to apply the most appropriate PA configuration. The main PA characteristic represented in these tables is the portion of the PA activated for each transmit power level. As the transmit power increases, a larger portion of the PA is applied. These tables are loaded into the SoC through a configuration file during firmware initialization.

Having discussed the key aspects of IMD3 and its mitigation techniques in the above sections, it is important to reflect on the overall implications of this study. In this project the complete implementation of the IMD3 mitigation techniques is carried out using a Python-based program. A detailed explanation of this tool is provided in the following chapter. The program takes IMD3 measurement data as input, performs analysis based on critical parameters, makes arbitration decisions, determines appropriate feedback power levels for each radio, and finally generates output in the form of register settings. These settings can be directly applied to the hardware through a corresponding firmware script.

CHAPTER 4

IMPLEMENTATION OF IMD3 MITIGATION TECHNIQUES USING PYTHON-BASED AUTOMATION

The IMD3 performance of a multi-radio chipset depends on variations in the transmit power levels of the coexisting radios. Consequently, IMD3 measurements are primarily conducted across a range of WLAN and Bluetooth transmit power combinations. In addition to power levels, other influencing factors further define the test cases used for IMD3 characterization.

In this project, IMD3 levels are measured for a comprehensive set of parameter combinations. These include frequency separations categorized as high, medium, and low; WLAN modulation schemes such as 802.11b and 802.11n; Bluetooth radio types including BTC (BR/EDR) and BLE; the two configuration tables IMD3 optimized, and efficiency based and different antenna isolation levels. When the IMD3 measurement data from all parameter combinations are aggregated, it results in a significantly large dataset. Furthermore, the dataset size effectively doubles, as each parameter combination is evaluated separately for IMD3 measurements at both radio PAs.

Implementing IMD3 mitigation techniques on such a large dataset is highly impractical through manual processing. The likelihood of human error increases, and the analysis becomes time-consuming and inefficient. To address this challenge, a dedicated tool was developed using the Python programming language. This tool is designed to efficiently analyze the IMD3 measurement data and generate results corresponding to the two proposed mitigation techniques. This chapter gives a detailed structure of the designed Python program.

4.1 Tool Algorithm

This section outlines the structured approach used to implement the complete Python-based solution. The flowchart shown in Figure 4.1 illustrates the overall implementation flow, starting from the input IMD3 measurement data to the generation of final register settings.

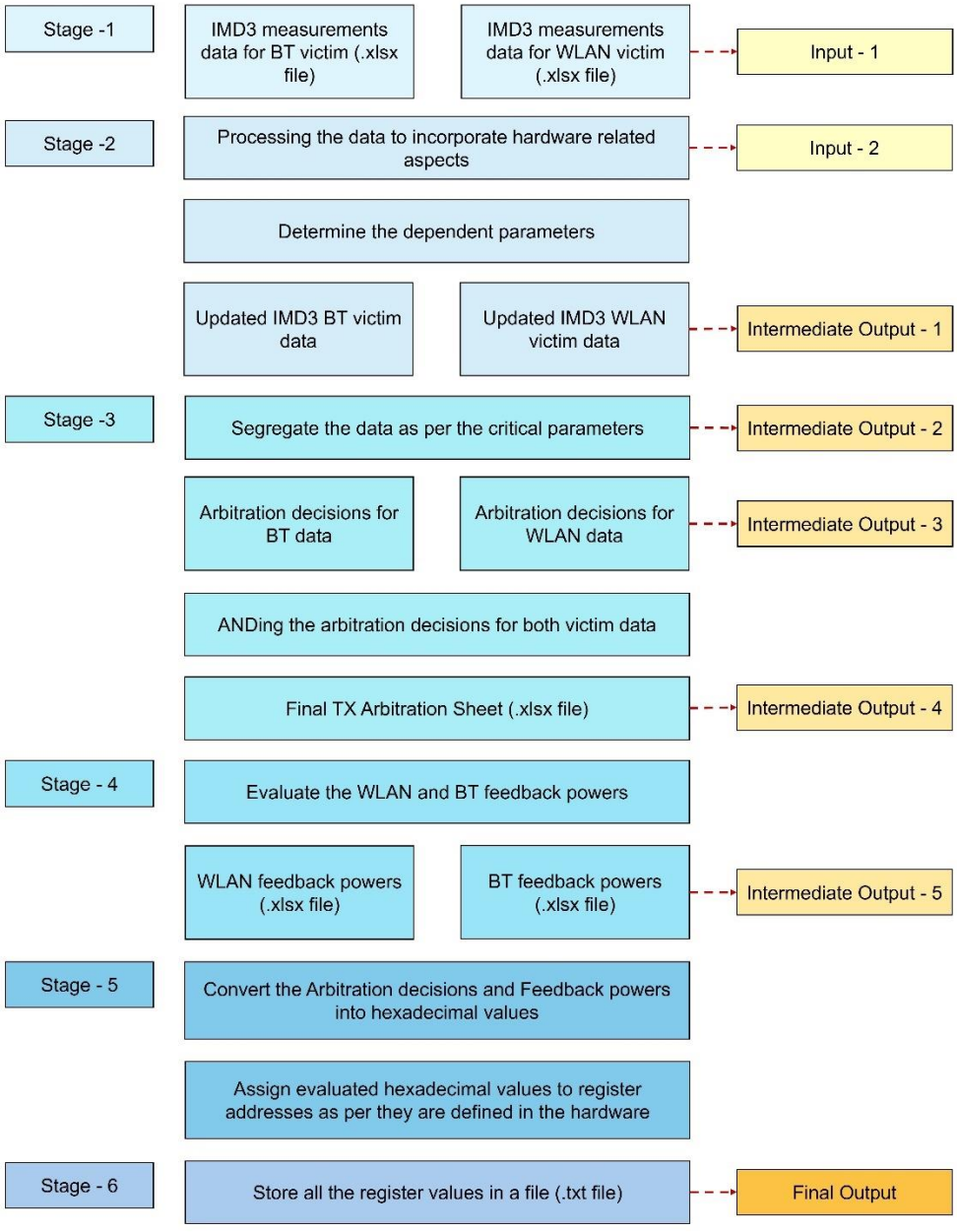
Stage -1
IMD3 measurements data for BT victim (.xlsx file)
IMD3 measurements data for WLAN victim (.xlsx file)
Input - 1
Stage -2
Processing the data to incorporate hardware related aspects
Input - 2
Determine the dependent parameters
Updated IMD3 BT victim data
Updated IMD3 WLAN victim data
Intermediate Output - 1
Stage -3
Segregate the data as per the critical parameters
Intermediate Output - 2
Arbitration decisions for BT data
Arbitration decisions for WLAN data
Intermediate Output - 3
ANDing the arbitration decisions for both victim data
Final TX Arbitration Sheet (.xlsx file)
Intermediate Output - 4
Stage - 4
Evaluate the WLAN and BT feedback powers
WLAN feedback powers (.xlsx file)
BT feedback powers (.xlsx file)
Intermediate Output - 5
Stage - 5
Convert the Arbitration decisions and Feedback powers into hexadecimal values
Assign evaluated hexadecimal values to register addresses as per they are defined in the hardware
Stage - 6
Store all the register values in a file (.txt file)
Final Output

Figure 4.1: Complete Algorithm for Python Based Implementation of IMD3 Mitigation Techniques

After implementing all the stages in sequence, the tool is capable of analyzing and applying both TX arbitration and power backoff techniques to any IMD3 dataset, regardless of the measurement parameters involved. Each stage of the process is described in detail in the following subsections.

4.1.1 Stage 1: Input to the Automation Tool

The automation tool takes two Excel files as input. Each file contains IMD3 measurement data where one of the radios is considered the victim. These files include IMD3 values for different combinations of key parameters. The path to these files are provided as input to the Python code for processing.

Each input sheet contains an extensive dataset with a large number of IMD3 measurement points. Assuming WLAN supports a transmit power range from 0 dBm to 20 dBm and Bluetooth supports transmit powers from -20 dBm to 20 dBm, the total number of IMD3 measurement combinations accounts to 800. When measurements are extended to three different channel combinations, corresponding to three distinct frequency separations, the total increases to 2,400 data points. Further, considering BTC with both BR and EDR data rates, the count doubles to 4,800. If measurements are also taken across a minimum of five different antenna isolation levels, the dataset expands to 24,000 points. And finally for two configuration tables the number of measurement points will rise to 48,000.

Notably, this Figure accounts for measurements taken at only one PA. When the measurements for the second PA are included, the total number of data points rises to 96,000. The input Excel files contain datasets in which the IMD3 level is recorded for every possible combination of the seven influencing parameters.

The following tables 4.1 and table 4.2 show a part of the input Excel files with IMD3 measurements at WLAN and Bluetooth victim (respective PA) respectively.

Table 4.1: Input Raw Data - Measured IMD3 levels for WLAN Victim with respect to Influencing Parameters

Test Name	Config. File name	WLAN radio			Bluetooth radio			Attenuati-on (dB)	IMD3 level (dBm)
		Channel_freq (MHz)	Modulation	setPower (dBm)	Channel_freq (MHz)	Data rate	setPower (dBm)		
WL victim	Eff.txt	2472	802.11b	2	2438	BR	-19	15	-40.6
WL victim	Eff.txt	2472	802.11n	7	2438	EDR	-14	15	-41.1
WL victim	Eff.txt	2472	802.11b	13	2446	BR	-11	20	-43.2
WL victim	IMD.txt	2472	802.11n	16	2446	EDR	7	20	-38.4
WL victim	IMD.txt	2472	802.11b	19	2456	BR	13	25	-39.7
WL victim	IMD.txt	2472	802.11n	20	2456	EDR	18	25	-40.5

Table 4.2: Input Raw Data - Measured IMD3 levels for Bluetooth Victim with respect to Influencing Parameters

Test Name	Config. File name	WLAN radio			Bluetooth radio			Attenuati-on (dB)	IMD3 level (dBm)
		Channel_freq (MHz)	Modulation	setPower (dBm)	Channel_freq (MHz)	Data rate	setPower (dBm)		
BT victim	Eff.txt	2472	802.11b	5	2438	BR	-18	15	-40.7
BT victim	Eff.txt	2472	802.11n	8	2438	EDR	-15	15	-39.5
BT victim	Eff.txt	2472	802.11b	11	2446	BR	-10	20	-43.9
BT victim	IMD.txt	2472	802.11n	14	2446	EDR	6	20	-46.5
BT victim	IMD.txt	2472	802.11b	17	2456	BR	12	25	-41.2
BT victim	IMD.txt	2472	802.11n	20	2456	EDR	19	25	-46.3

In the above tables the 'Test Name' column indicates the measurement scenario, highlighting the victim radio. The 'Configuration File Name' specifies which configuration file was loaded

along with the firmware which then indicates the configuration table loaded into the SoC. All remaining columns contain data corresponding to their respective headers.

4.1.2 Stage 2: Post Processing of the Raw Data

The second stage involves processing the raw measurement data to include hardware-related parameters and to derive additional analytical fields. Key hardware aspects, such as front-end loss and conducted path loss, are considered. New parameters are also calculated, including the frequency difference between the transmit channels, which is then categorized as high, medium, or low separation. The actual isolation between the two transmitting antennas is determined by adding the conducted path loss to the attenuation value. Additionally, a column indicating the configuration table used is appended, based on the configuration file name provided in the input data.

Arbitration decisions are also made in this stage based on the measured IMD3 levels. The tool provides an option to apply a tighter threshold than the original FCC IMD3 specification by introducing an additional margin of 3–4 dB. This added buffer accounts for run-to-run variations and other potential sources of measurement or system-level inaccuracies, ensuring more robust decision-making.

In addition to the IMD3 measurement data, other parameters required for post processing are provided as inputs at this stage. These parameters are included in a separate Excel file, which is read by the Python program at the beginning of execution. Table 4.3 lists the fields present in the Input Excel file.

Table 4.3: Input Parameters given at Stage 2

Sr. No.	Parameter Field	Parameter Value
1	Path to WLAN victim data	file_path_WLAN.xlsx
2	Path to Bluetooth victim data	file_path_Bluetooth.xlsx
3	FE loss for WLAN antenna	1 dB
4	FE loss for Bluetooth antenna	1 dB
5	Insertion Loss (Path loss)	8 dB
6	Additional margin to the regulatory spec	3 dB
7	Ranges for frequency separation	High = 34 MHz Medium = 26 MHz Low = 16 MHz
8	Configuration file name for efficiency optimized configuration table	Eff.txt

Based on these input fields read from the input Excel file, the results are computed and stored in new columns that are appended to the existing data sheets. The flowchart shown in Figure 4.2 illustrates the evaluations performed in the second stage. All blocks highlighted in green represent the new fields added to the original dataset.

The front-end loss is included to compensate for the difference between the measured power at the chip pin and at the antenna. This difference arises due to the presence of intermediate components in the signal path on the SoC, which introduce a significant loss.

The insertion loss or path loss, on the other hand, is considered to ensure accurate estimation of the isolation between the two transmitting antennas. This includes the attenuation introduced by the physical attenuator, as well as the cumulative losses from measurement devices and connecting cables used in the IMD3 measurement setup.

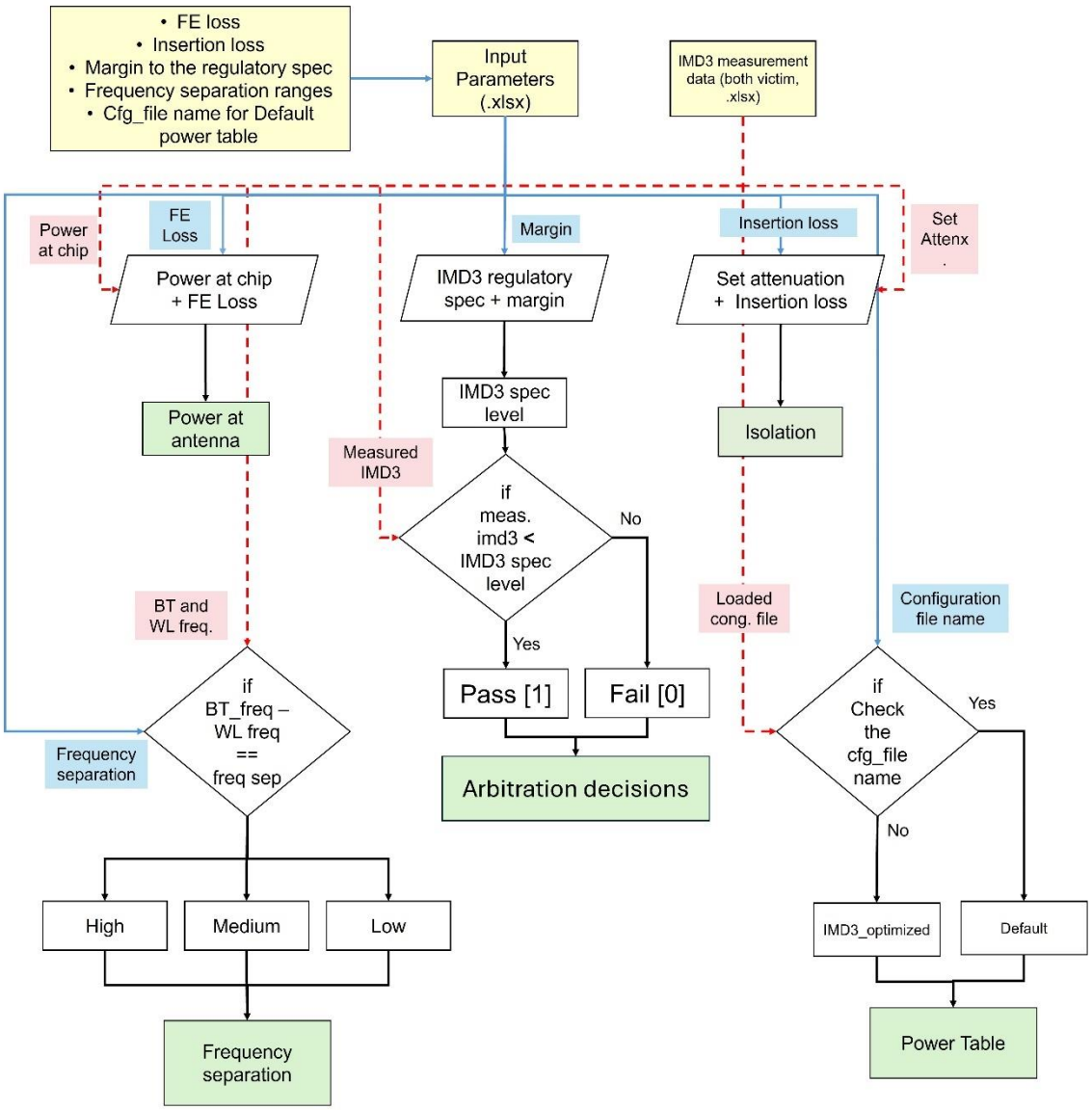

Figure 4.2: Flowchart Representing Derivation of Additional Fields from the Raw Input Data

4.1.3 Stage 3: Organization of Data and TX Arbitration Sheet Generation

After completing all the post-processing steps on the raw data, a refined dataset is generated. The next step in the implementation is data segregation. As previously discussed, IMD3 measurements are available for all possible combinations of WLAN and Bluetooth transmit

power levels, and arbitration decisions have already been made for each case in the earlier stage.

However, directly converting these arbitration decisions into hexadecimal register values would require a large number of hardware registers due to their limited size. This would lead to high memory usage, which is not cost-effective. To address this, the full range of WLAN and Bluetooth power levels is divided into eight regions, known as bins. Each bin is represented by a power level that exhibits the worst IMD3 performance within that subrange. As a result, only 64 representative power combinations (8 WLAN bins × 8 Bluetooth bins) are selected to generate the final arbitration sheet.

Figure 4.3 provides a simplified illustration of how the Bluetooth transmit power range is divided into eight bins and the corresponding table 4.4 shows how representative values are selected for each bin. The plot displays the measured IMD3 levels against the Bluetooth transmit power and represents the IMD3 characteristics for the specific chipset under evaluation.

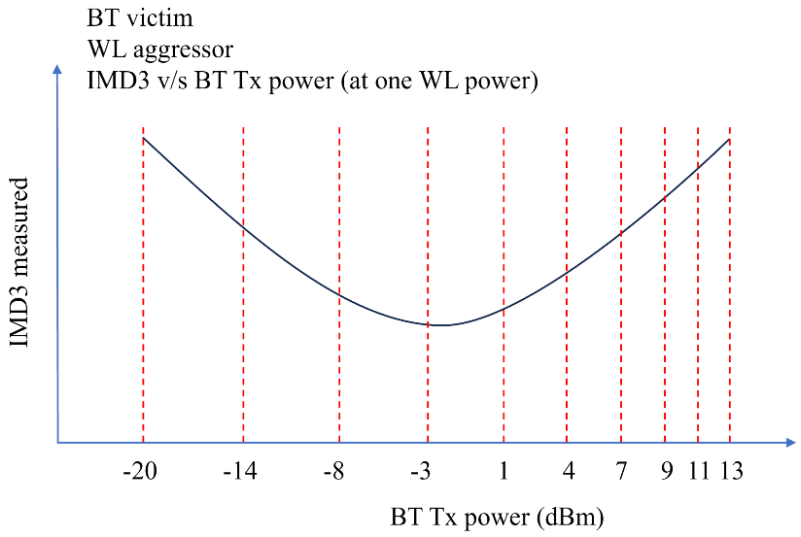

Figure 4.3: Division of Complete Bluetooth TX Power Range into Eight Bins

Table 4.4: Bluetooth Bins and their Respective Power Bin Representatives

Bin no.	Minimum power	Maximum power	Bin representative
1	-20	-15	-20
2	-14	-9	-14
3	-8	-4	-8
4	-3	0	0
5	1	3	3
6	4	6	6
7	7	8	8
8	9	10	10

The complete updated dataset is segmented based on the influencing parameters, and the corresponding arbitration decisions are selected only for the power levels that serve as bin representatives. The flowchart in Figure 4.4 illustrates the segregation process, showing how the full dataset is filtered and organized according to specific parameter combinations for efficient arbitration table generation.

The entire post-processing and data segregation steps are performed separately for the WLAN and Bluetooth victim datasets. After segmenting the data based on the influencing parameters, two output sheets are generated, each containing a selected number of rows and columns. These sheets have the TX arbitration decisions corresponding to the IMD3 measurement data for WLAN and Bluetooth victims, respectively.

However, since both radios coexist on the same system, it is essential that regulatory specifications are not violated by either of them. To ensure this, a logical AND operation is performed between the arbitration decisions of the two radios. Before applying the AND operation, the correct arbitration decisions must be identified from both WLAN and Bluetooth victim data sheets under the same set of influencing parameters. This step requires careful matching of parameter combinations to ensure accurate alignment. The outcome is a final TX

arbitration sheet that accounts for the IMD3 performance of both radios simultaneously. Figure 4.5 shows a block representation of this.

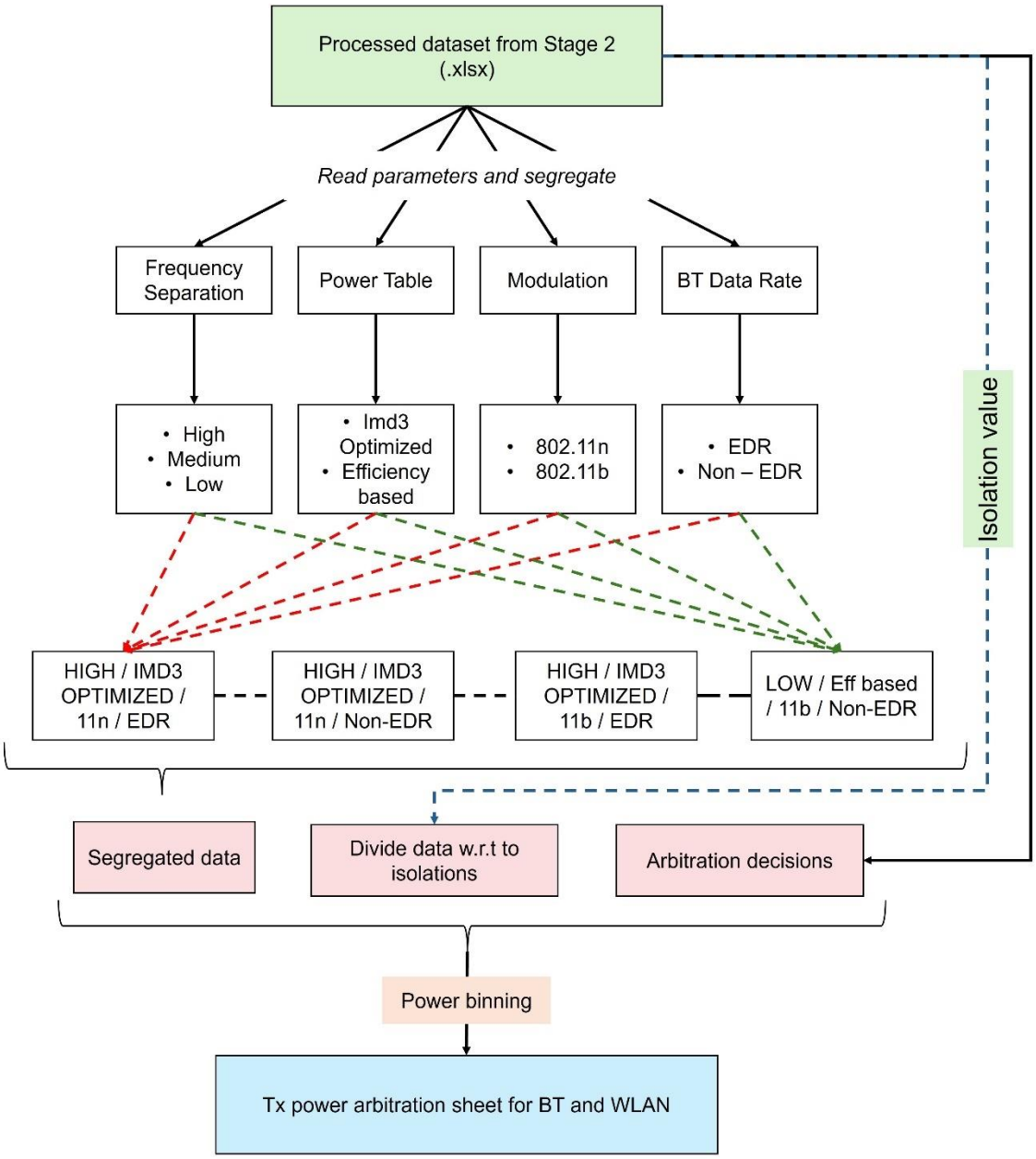
Processed dataset from Stage 2 (.xlsx)
Read parameters and segregate
Frequency Separation
Power Table
Modulation
BT Data Rate
• High • Medium • Low
• Imd3 Optimized • Efficiency based
• 802.11n • 802.11b
• EDR • Non – EDR
Isolation value
HIGH / IMD3 OPTIMIZED / 11n / EDR
HIGH / IMD3 OPTIMIZED / 11n / Non-EDR
HIGH / IMD3 OPTIMIZED / 11b / EDR
LOW / Eff based / 11b / Non-EDR
Segregated data
Divide data w.r.t to isolations
Arbitration decisions
Power binning
Tx power arbitration sheet for BT and WLAN

Figure 4.4: Flowchart Showing Segregation of Processed Data w.r.t Measurement Parameters

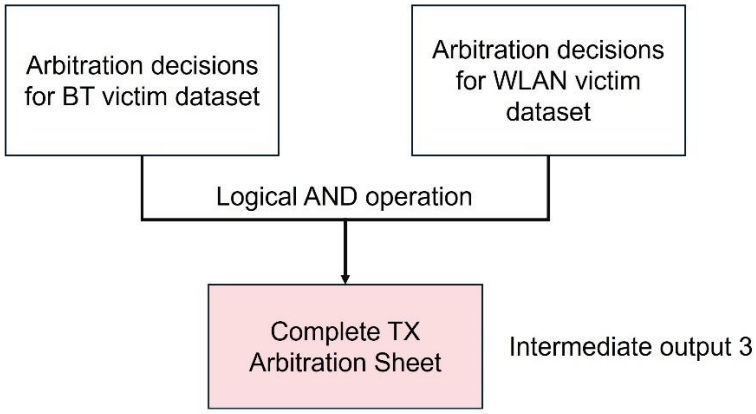
Arbitration decisions for BT victim dataset
Arbitration decisions for WLAN victim dataset
Logical AND operation
Complete TX Arbitration Sheet
Intermediate output 3

Figure 4.5: Block Diagram to Show Generation of Final TX Arbitration Sheet

4.1.4 Stage 4: Deriving WLAN and Bluetooth Feedback Powers

Once the arbitration decisions are made in binary form (1 for allowed, 0 for blocked), the next step involves determining the feedback power for the lower-priority radio. Since radio priority is defined by the requirements of the supported application, the tool is designed to compute feedback powers for both radios independently, assuming each one to be the lower-priority transmitter in separate iterations. This ensures flexibility in adapting to different application scenarios.

The logic used to determine the feedback powers is straightforward. This stage takes the final TX arbitration sheet, generated in the previous step, as input. The algorithm processes one parameter combination and one isolation level at a time. It scans through all arbitration decisions to detect transitions from '1' (allowed) to '0' (blocked). When such a transition is found, it records the corresponding power level of the lower-priority radio as the feedback power.

If all power levels for the lower-priority radio are allowed, the algorithm assigns the maximum power level as the feedback power. Conversely, if none of the combinations are allowed, it stores a special indicator value that instructs the hardware that concurrent transmission is not permitted for any power setting.

The logic for identifying the transition from arbitration decision '1' to '0' is illustrated in Figure 4.6 for better understanding. Consider a case where Bluetooth is the lower-priority radio, and the arbitration decisions are shown for a fixed WLAN transmit power level. All the highlighted cells represent the finalized feedback power values for Bluetooth in each case.

BT Tx power	Arbitration decision
-19	0
-17	0
-11	0
1	0
5	0
9	0
11	0
13	0

BT Tx power	Arbitration decision
-19	1
-17	1
-11	1
1	1
5	1
9	1
11	1
13	1

BT Tx power	Arbitration decision
-19	1
-17	1
-11	1
1	1
5	0
9	0
11	0
13	0

BT Tx power	Arbitration decision
-19	0
-17	0
-11	1
1	1
5	1
9	1
11	0
13	0

Figure 4.6: Logic for Identification of Feedback Power by the Algorithm

Figure 4.7 presents a simplified flowchart outlining the steps followed by the algorithm in this stage.

After evaluating the feedback powers for all scenarios, the results are stored in two separate output sheets, one for WLAN and one for Bluetooth. Each sheet corresponds to all measured parameter combinations. It is crucial to maintain accurate tracking of these parameters, as a large number of combinations are involved.

Furthermore, the feedback power must be correctly mapped to the respective high-priority radio power. If the feedback power is set lower than necessary for a fixed high-priority radio power level, it can lead to excessive power backoff, resulting in reduced overall system throughput. Conversely, if the feedback power is set higher than expected, it may lead to IMD3 failures. Therefore, accurate mapping and storage are essential to ensure both regulatory compliance and optimal performance.

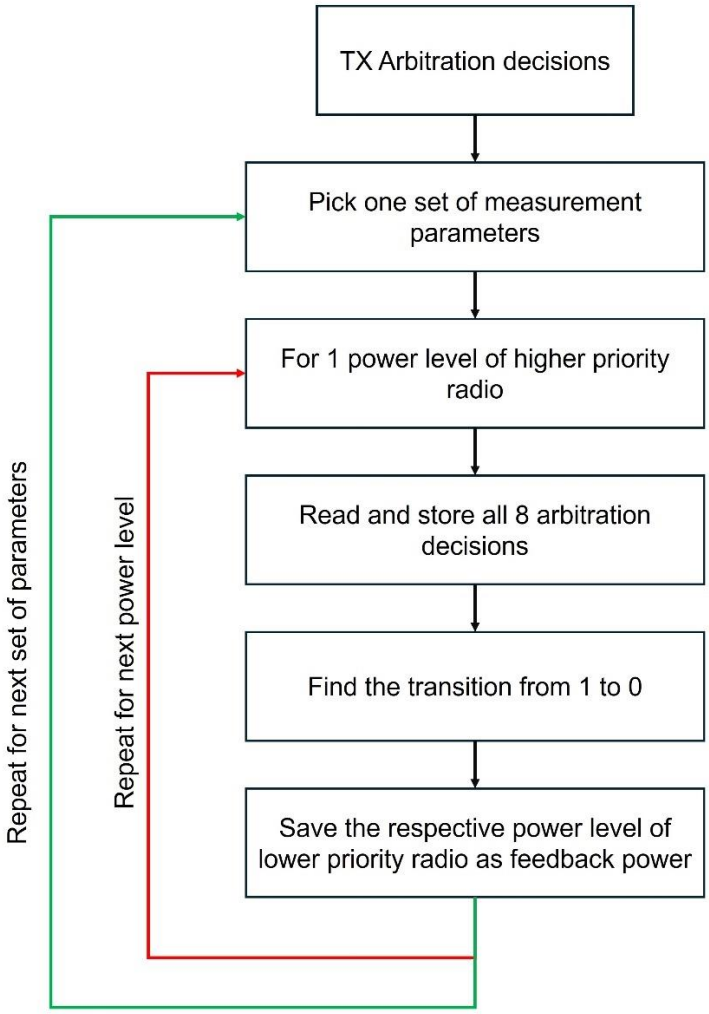
TX Arbitration decisions
Pick one set of measurement parameters
For 1 power level of higher priority radio
Read and store all 8 arbitration decisions
Find the transition from 1 to 0
Save the respective power level of lower priority radio as feedback power
Repeat for next power level
Repeat for next set of parameters

Figure 4.7: Flowchart Showing Process of Determining Feedback Powers for Lower Priority Radio

4.1.5 Stage 5: Evaluating the Register Values

Registers are fixed storage locations in the hardware memory used to store values that control specific hardware functionalities. Different sections of the register configuration range are used to map various combinations of parameters. For example, the first ten registers might be

dedicated for storing arbitration decisions for high frequency separation, 802.11n WLAN modulation, Bluetooth BR data rate, and 15 dB isolation.

If incorrect values are written to the registers, the hardware will not function properly for that specific configuration. Even if the evaluated values are correct, writing them to the wrong register addresses can cause the hardware to behave incorrectly. Therefore, correctly assigning the evaluated values is a very critical aspect of this stage.

For the chipsets that were considered in the course of this project has registers of size 32 bits each to store the arbitration decisions and feedback powers. In the case of TX arbitration, the decisions are already in terms of 1 and 0. Depending on the register definitions in the hardware, the arbitration decisions are arranged in a long binary string. These are then divided into chunks of 32 bits each, which are converted to 8-byte hexadecimal values. Figure 4.8 illustrates these steps through a flowchart.

Evaluating register settings for TX arbitration is relatively straightforward. The main challenge lies in accurately assigning these settings to the correct register addresses. To achieve this, the algorithm uses three Python dictionaries. The first dictionary maps the evaluated arbitration values to their corresponding parameter sets from the TX arbitration sheet. The second dictionary maps hardware-defined register addresses to their respective parameter sets as per the hardware definition. The algorithm then matches the parameter sets from both dictionaries and assigns the evaluated values to the correct register addresses using a third dictionary. This process is illustrated in the simplified diagram shown in Figure 4.9.

Based on the configurations supported by a chipset, the corresponding registers are predefined in the hardware. The tool applies this logic to accurately evaluate and assign register values for all supported parameter sets. The algorithm takes the starting and ending register addresses as input, generates an array of addresses, and assigns the evaluated values accordingly.

The next set of registers are used for storing WLAN and Bluetooth feedback power values. The chipset includes separate registers for each radio when they operate with lower priority. In this case, all feedback power values, read from the feedback power sheets from the previous stage, are stored in an array, following the sequence defined by the chipset's register layout.

This sequence mainly depends on the order of WLAN and Bluetooth modulations. It's important to note that register addresses remain unchanged regardless of isolation levels. Antenna isolation is determined based on the intended application and typically remains fixed once the application is defined.

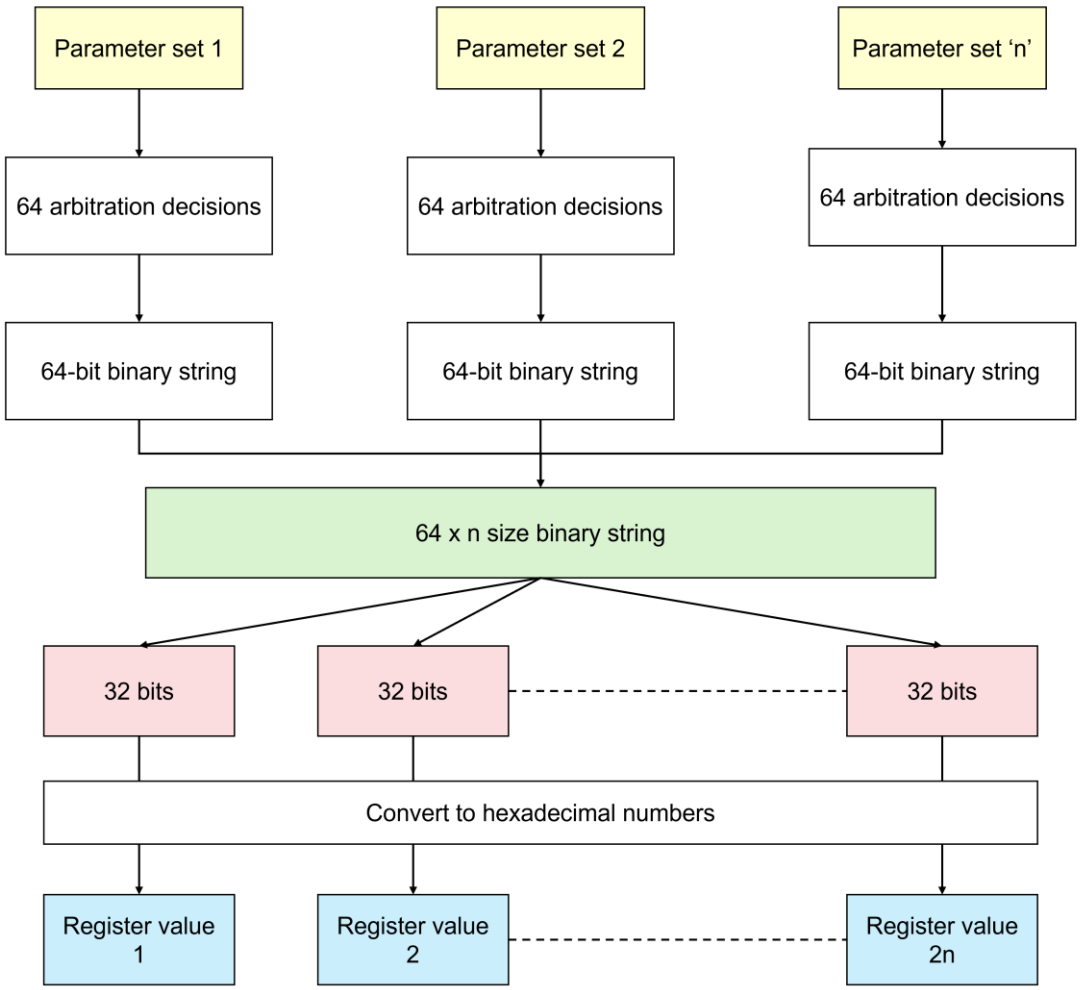

Figure 4.8: Evaluation of Hardware Register Values for TX Arbitration Technique

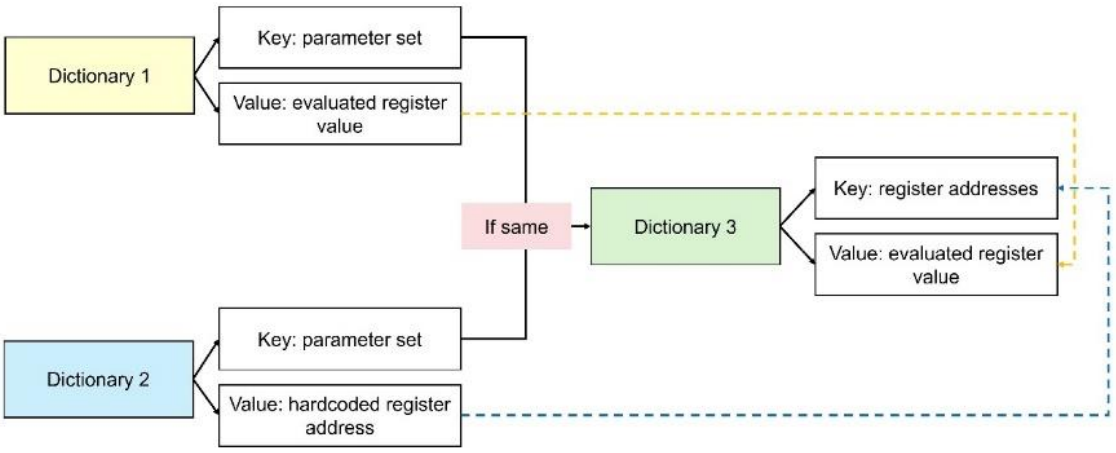

Figure 4.9: Assignment of Evaluated Register Values to Register Addresses as per Hardware Definition for TX Arbitration Technique

The power levels from this array are then converted into binary values. Since Bluetooth supports a wider range of transmit power levels, from -20 dBm to 20 dBm, 6 bits are used to represent all possible values. In contrast, WLAN supports a narrower range of 0 dBm to 20 dBm, which can be represented using 5-bit binary numbers. As a result, a long binary string is generated, following the order of the hardware register definitions for each radio respectively.

This string is then split into 32-bit segments. Each 32-bit segment is converted into an 8-character hexadecimal value. These computed values are then mapped to their corresponding register addresses using a Python dictionary. The algorithm ensures that the correct parameter set is matched, and the values are assigned appropriately. This process is then repeated for different isolation levels.

Figure 4.10 presents a simplified flowchart that illustrates the steps involved in obtaining the register values for feedback powers for one cycle of a fixed antenna isolation.

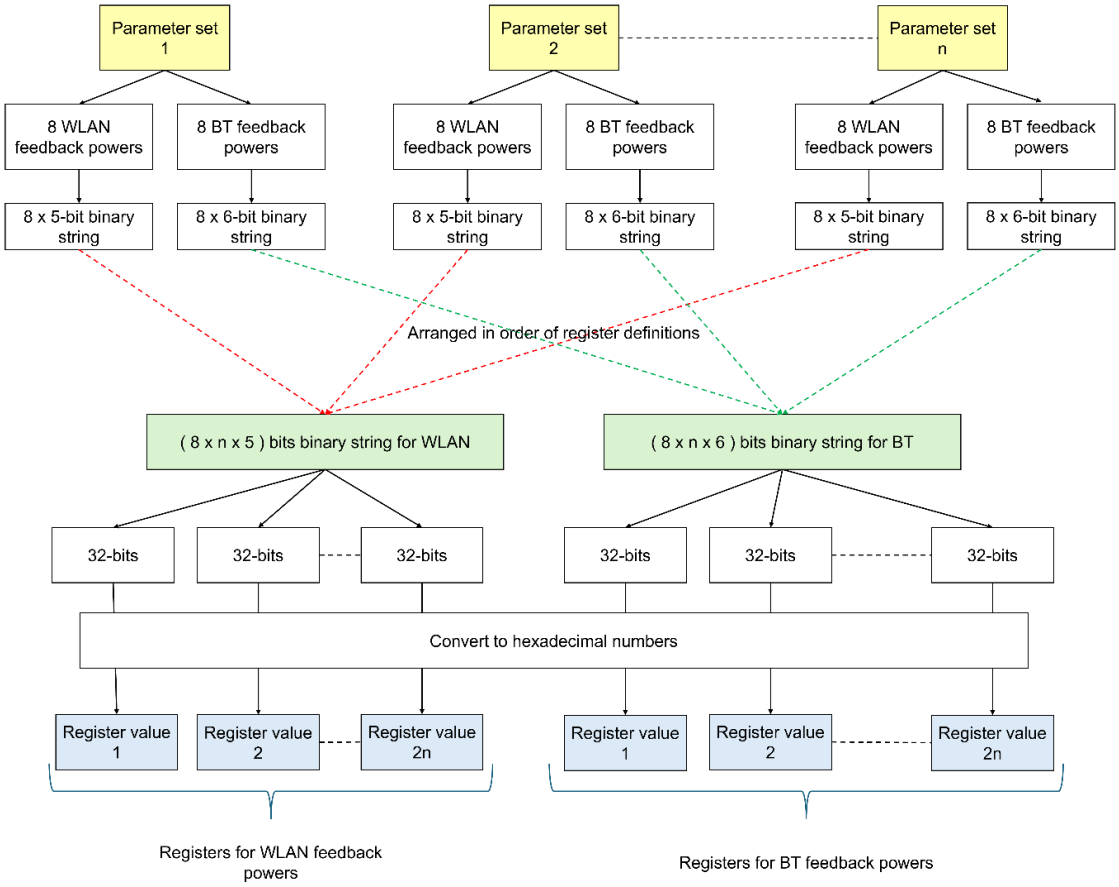
Parameter set 1
Parameter set 2
Parameter set n
8 WLAN feedback powers
8 BT feedback powers
8 WLAN feedback powers
8 BT feedback powers
8 WLAN feedback powers
8 BT feedback powers
8 x 5-bit binary string
8 x 6-bit binary string
8 x 5-bit binary string
8 x 6-bit binary string
8 x 5-bit binary string
8 x 6-bit binary string
Arranged in order of register definitions
(8 x n x 5) bits binary string for WLAN
(8 x n x 6) bits binary string for BT
32-bits
32-bits
32-bits
32-bits
32-bits
32-bits
Convert to hexadecimal numbers
Register value 1
Register value 2
Register value 2n
Register value 1
Register value 2
Register value 2n
Registers for WLAN feedback powers
Registers for BT feedback powers

Figure 4.10: Evaluation of Hardware Register Values for Power Backoff Technique

This is how the register values for both mitigation techniques are evaluated and stored, each mapped to its corresponding register address. As a result, two distinct sets of registers are generated at the output of this stage.

4.1.6 Stage 6: Storing the Register Values in the Output File

This final stage of the algorithm involves compiling all register addresses along with their corresponding values into a predefined format. To reduce the possibility of manual errors, the algorithm automatically saves the register information in a chipset-specific format compatible

for direct use by the firmware. The output of this stage is a text file containing all the necessary register details.

The developed Python program is designed to efficiently handle large datasets with various combinations of measurement parameters. Only the parameters that may vary between runs are provided as input to the tool. The rest of the analysis and result generation is fully automated by the program. The results produced at each stage are presented in the following chapter.

CHAPTER 5

RESULTS AND CONCLUSION

This chapter presents the results obtained from the Python-based implementation of the two mitigation techniques: TX arbitration and power backoff. It provides a detailed explanation of each intermediate output generated during the process. The chapter concludes with a summary of the key findings and offers insights into possible directions for future research and improvement.

5.1 Results of the Python Automation Tool

As outlined in the previous chapter, the automation tool follows a multi-stage algorithm, generating several intermediate results throughout the process. The final output, produced at the end of the sixth stage, is a text file containing all the register settings. This section presents the results obtained at each stage, corresponding to the steps illustrated in Figure 4.1. In total, the tool generates nine Excel sheets and one text file upon execution. Figure 5.1 provides a consolidated summary of all these outputs.

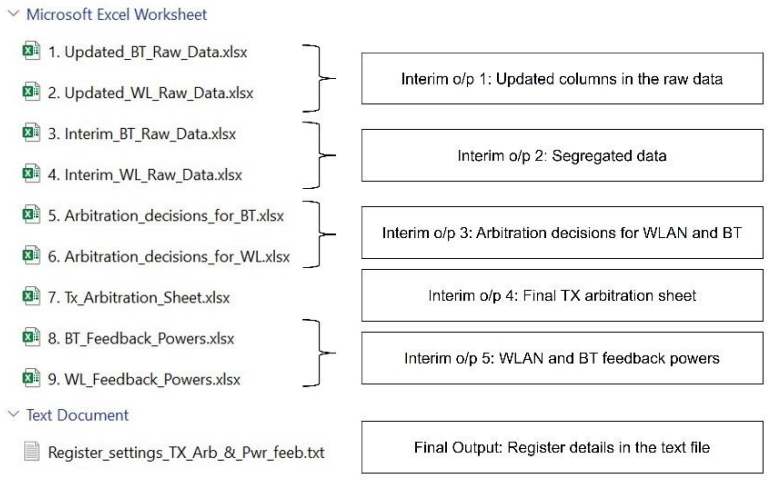

Figure 5.1: Output Files Generated by the Python Based Implementation Tool

5.1.1 Stage 1: Raw Input Data for Automation Processing

Input to the automation tool are the measured IMD3 levels at WLAN and Bluetooth PA side with respect to all the influencing parameters. A part of this data is shown in the following Figure 5.2 and 5.3 for WLAN victim and Bluetooth victim respectively.

	A	B	C	D	E	F	G	H	I	J
1	**testName**	**cfgFile**	**WLAN freq(MHz)**	**WLAN modulation**	**WLAN setPwr**	**BT_DataRate**	**BT_Freq (MHz)**	**btSet**	**AttenX**	**IMD**
2	WL Vict_IMD3	IMD3.txt	2472	802.11n	0	BR	2438	-20	10	-52.8
3	WL Vict_IMD3	IMD3.txt	2472	802.11n	0	BR	2438	-19	10	-52.9
4	WL Vict_IMD3	IMD3.txt	2472	802.11n	0	BR	2438	-18	10	-54.1
5	WL Vict_IMD3	IMD3.txt	2472	802.11n	0	BR	2438	-17	10	-53.6
6	WL Vict_IMD3	IMD3.txt	2472	802.11n	0	BR	2438	-16	10	-51.2
7	WL Vict_IMD3	IMD3.txt	2472	802.11n	0	BR	2438	-15	10	-50.3
8	WL Vict_IMD3	IMD3.txt	2472	802.11n	0	BR	2446	-14	10	-48.3
9	WL Vict_IMD3	IMD3.txt	2472	802.11n	0	BR	2446	-13	10	-47.3
10	WL Vict_IMD3	IMD3.txt	2472	802.11n	0	BR	2446	-12	10	-46.8
11	WL Vict_IMD3	Eff.txt	2472	802.11b	0	BR	2446	-11	10	-49.2
12	WL Vict_IMD3	Eff.txt	2472	802.11b	0	BR	2446	-10	10	-47.1
13	WL Vict_IMD3	Eff.txt	2472	802.11b	0	BR	2446	-9	10	-47.7
14	WL Vict_IMD3	Eff.txt	2472	802.11b	0	BR	2446	-8	10	-47.3
15	WL Vict_IMD3	Eff.txt	2472	802.11b	0	BR	2446	-7	10	-47.2
16	WL Vict_IMD3	Eff.txt	2472	802.11b	0	BR	2456	-6	10	-47.6
17	WL Vict_IMD3	Eff.txt	2472	802.11b	0	BR	2456	-5	10	-46.4
18	WL Vict_IMD3	Eff.txt	2472	802.11b	0	BR	2456	-4	10	-46.0
19	WL Vict_IMD3	Eff.txt	2472	802.11b	0	BR	2456	-3	10	-46.1
20	WL Vict_IMD3	Eff.txt	2472	802.11b	0	BR	2456	-2	10	-45.4

Figure 5.2: WLAN Victim IMD3 Measurement Input Data for The Automation Tool

	A	B	C	D	E	F	G	H	I	J
1	testName	cfgFile	WLAN freq(MHz)	WLAN modulation	WLAN setPwr	BT_DataRate	BT_Freq (MHz)	btSet	AttenX	IMD
2	BT Vict_IMD3	IMD3.txt	2472	802.11n	0	BR	2438	-20	10	-53.6
3	BT Vict_IMD3	IMD3.txt	2472	802.11n	0	BR	2438	-19	10	-53.9
4	BT Vict_IMD3	IMD3.txt	2472	802.11n	0	BR	2438	-18	10	-52.5
5	BT Vict_IMD3	IMD3.txt	2472	802.11n	0	BR	2438	-17	10	-51.0
6	BT Vict_IMD3	IMD3.txt	2472	802.11n	0	BR	2438	-16	10	-49.7
7	BT Vict_IMD3	IMD3.txt	2472	802.11n	0	BR	2438	-15	10	-48.1
8	BT Vict_IMD3	IMD3.txt	2472	802.11n	0	BR	2446	-14	10	-48.0
9	BT Vict_IMD3	IMD3.txt	2472	802.11n	0	BR	2446	-13	10	-50.4
10	BT Vict_IMD3	IMD3.txt	2472	802.11n	0	BR	2446	-12	10	-48.0
11	BT Vict_IMD3	Eff.txt	2472	802.11b	0	BR	2446	-11	10	-49.2
12	BT Vict_IMD3	Eff.txt	2472	802.11b	0	BR	2446	-10	10	-48.1
13	BT Vict_IMD3	Eff.txt	2472	802.11b	0	BR	2446	-9	10	-48.2
14	BT Vict_IMD3	Eff.txt	2472	802.11b	0	BR	2446	-8	10	-48.2
15	BT Vict_IMD3	Eff.txt	2472	802.11b	0	BR	2446	-7	10	-47.5
16	BT Vict_IMD3	Eff.txt	2472	802.11b	0	BR	2456	-6	10	-46.9
17	BT Vict_IMD3	Eff.txt	2472	802.11b	0	BR	2456	-5	10	-47.3
18	BT Vict_IMD3	Eff.txt	2472	802.11b	0	BR	2456	-4	10	-46.8
19	BT Vict_IMD3	Eff.txt	2472	802.11b	0	BR	2456	-3	10	-43.1
20	BT Vict_IMD3	Eff.txt	2472	802.11b	0	BR	2456	-2	10	-43.5

Figure 5.3: Bluetooth Victim IMD3 Measurement Input Data for the Automation Tool

5.1.2 Stage 2: Output After Data Post-Processing

At this stage, the output comprises two Excel files containing additional columns, generated after processing and appending the analytical fields. Figure 5.4 and 5.5 illustrate sample outputs for both WLAN and Bluetooth victim scenarios.

	A	B	C	D	E	F	G	H	I	J	K	L	M	N	O	P	Q
1	testName	cfgFile	WLAN freq(MHz)	WLAN modulation	WLAN setPwr	BT_Data Rate	BT_Freq (MHz)	btSet	AttenX	IMD	BT_Tx	WL_Tx	Isolation	Power_table	Frequency_ difference	Frequency_ separation	Pass/Fail _INT
2	WL Vict_IMD3	IMD3.txt	2472	802.11n	0	BR	2438	-20	10	-52.8	-19	1	15	IMD3_Optimized	34	HIGH	1
3	WL Vict_IMD3	IMD3.txt	2472	802.11n	0	BR	2438	-19	10	-52.9	-18	1	15	IMD3_Optimized	34	HIGH	1
4	WL Vict_IMD3	IMD3.txt	2472	802.11n	0	BR	2438	-18	10	-54.1	-17	1	15	IMD3_Optimized	34	HIGH	1
5	WL Vict_IMD3	IMD3.txt	2472	802.11n	0	BR	2438	-17	10	-53.6	-16	1	15	IMD3_Optimized	34	HIGH	1
6	WL Vict_IMD3	IMD3.txt	2472	802.11n	0	BR	2438	-16	10	-51.2	-15	1	15	IMD3_Optimized	34	HIGH	1
7	WL Vict_IMD3	IMD3.txt	2472	802.11n	0	BR	2438	-15	10	-50.3	-14	1	15	IMD3_Optimized	34	HIGH	1
8	WL Vict_IMD3	IMD3.txt	2472	802.11n	0	BR	2446	-14	10	-48.3	-13	1	15	IMD3_Optimized	26	MEDIUM	1
9	WL Vict_IMD3	IMD3.txt	2472	802.11n	0	BR	2446	-13	10	-47.3	-12	1	15	IMD3_Optimized	26	MEDIUM	1
10	WL Vict_IMD3	IMD3.txt	2472	802.11n	0	BR	2446	-12	10	-46.8	-11	1	15	IMD3_Optimized	26	MEDIUM	1
11	WL Vict_IMD3	Eff.txt	2472	802.11b	0	BR	2446	-11	10	-49.2	-10	1	15	Efficiency based	26	MEDIUM	1
12	WL Vict_IMD3	Eff.txt	2472	802.11b	0	BR	2446	-10	10	-47.1	-9	1	15	Efficiency based	26	MEDIUM	1
13	WL Vict_IMD3	Eff.txt	2472	802.11b	0	BR	2446	-9	10	-47.7	-8	1	15	Efficiency based	26	MEDIUM	1
14	WL Vict_IMD3	Eff.txt	2472	802.11b	0	BR	2446	-8	10	-47.3	-7	1	15	Efficiency based	26	MEDIUM	1
15	WL Vict_IMD3	Eff.txt	2472	802.11b	0	BR	2446	-7	10	-47.2	-6	1	15	Efficiency based	26	MEDIUM	1
16	WL Vict_IMD3	Eff.txt	2472	802.11b	0	BR	2456	-6	10	-47.6	-5	1	15	Efficiency based	16	LOW	1
17	WL Vict_IMD3	Eff.txt	2472	802.11b	0	BR	2456	-5	10	-46.4	-4	1	15	Efficiency based	16	LOW	1
18	WL Vict_IMD3	Eff.txt	2472	802.11b	0	BR	2456	-4	10	-46.0	-3	1	15	Efficiency based	16	LOW	1
19	WL Vict_IMD3	Eff.txt	2472	802.11b	0	BR	2456	-3	10	-46.1	-2	1	15	Efficiency based	16	LOW	1
20	WL Vict_IMD3	Eff.txt	2472	802.11b	0	BR	2456	-2	10	-45.4	-1	1	15	Efficiency based	16	LOW	1

Figure 5.4: WLAN Processed Data with Updated Columns

	A	B	C	D	E	F	G	H	I	J	K	L	M	N	O	P	Q
1	testName	cfgFile	WLAN freq(MHz)	WLAN modulation	WLAN setPwr	BT_Data Rate	BT_Freq (MHz)	btSet	AttenX	IMD	BT_Tx	WL_Tx	Isolation	Power_table	Frequency_ difference	Frequency_ separation	Pass/Fail _INT
2	BT Vict_IMD3	IMD3.txt	2472	802.11n	0	BR	2438	-20	10	-53.6	-19	1	15	IMD3_Optimized	34	HIGH	1
3	BT Vict_IMD3	IMD3.txt	2472	802.11n	0	BR	2438	-19	10	-53.9	-18	1	15	IMD3_Optimized	34	HIGH	1
4	BT Vict_IMD3	IMD3.txt	2472	802.11n	0	BR	2438	-18	10	-52.5	-17	1	15	IMD3_Optimized	34	HIGH	1
5	BT Vict_IMD3	IMD3.txt	2472	802.11n	0	BR	2438	-17	10	-51.0	-16	1	15	IMD3_Optimized	34	HIGH	1
6	BT Vict_IMD3	IMD3.txt	2472	802.11n	0	BR	2438	-16	10	-49.7	-15	1	15	IMD3_Optimized	34	HIGH	1
7	BT Vict_IMD3	IMD3.txt	2472	802.11n	0	BR	2438	-15	10	-48.1	-14	1	15	IMD3_Optimized	34	HIGH	1
8	BT Vict_IMD3	IMD3.txt	2472	802.11n	0	BR	2446	-14	10	-48.0	-13	1	15	IMD3_Optimized	26	MEDIUM	1
9	BT Vict_IMD3	IMD3.txt	2472	802.11n	0	BR	2446	-13	10	-50.4	-12	1	15	IMD3_Optimized	26	MEDIUM	1
10	BT Vict_IMD3	IMD3.txt	2472	802.11n	0	BR	2446	-12	10	-48.0	-11	1	15	IMD3_Optimized	26	MEDIUM	1
11	BT Vict_IMD3	Eff.txt	2472	802.11b	0	BR	2446	-11	10	-49.2	-10	1	15	Efficiency based	26	MEDIUM	1
12	BT Vict_IMD3	Eff.txt	2472	802.11b	0	BR	2446	-10	10	-48.1	-9	1	15	Efficiency based	26	MEDIUM	1
13	BT Vict_IMD3	Eff.txt	2472	802.11b	0	BR	2446	-9	10	-48.2	-8	1	15	Efficiency based	26	MEDIUM	1
14	BT Vict_IMD3	Eff.txt	2472	802.11b	0	BR	2446	-8	10	-48.2	-7	1	15	Efficiency based	26	MEDIUM	1
15	BT Vict_IMD3	Eff.txt	2472	802.11b	0	BR	2446	-7	10	-47.5	-6	1	15	Efficiency based	26	MEDIUM	1
16	BT Vict_IMD3	Eff.txt	2472	802.11b	0	BR	2456	-6	10	-46.9	-5	1	15	Efficiency based	16	LOW	1
17	BT Vict_IMD3	Eff.txt	2472	802.11b	0	BR	2456	-5	10	-47.3	-4	1	15	Efficiency based	16	LOW	1
18	BT Vict_IMD3	Eff.txt	2472	802.11b	0	BR	2456	-4	10	-46.8	-3	1	15	Efficiency based	16	LOW	1
19	BT Vict_IMD3	Eff.txt	2472	802.11b	0	BR	2456	-3	10	-43.1	-2	1	15	Efficiency based	16	LOW	1
20	BT Vict_IMD3	Eff.txt	2472	802.11b	0	BR	2456	-2	10	-43.5	-1	1	15	Efficiency based	16	LOW	1

Figure 5.5: Bluetooth Processed Data with Updated Columns

5.1.3 Stage 3: Output after Data Organization and TX Arbitration

The updated data sheets are then organized according to the influencing parameters and the selected WLAN and Bluetooth power levels. Figure 5.6 presents a snippet of WLAN sorted dataset.

	A	B	C	D	E	F	G	H
1	WL_Tx	BT_Tx	WLAN_mod ulation	BT_DataRate	Pass/Fail_WL_INT	Isolation	Frequency_separation	Power_table
2	1	-15	802.11b	BR	1	15	HIGH	Efficiency based
3	1	-5	802.11b	BR	1	15	HIGH	Efficiency based
4	1	0	802.11b	BR	1	15	HIGH	Efficiency based
5	1	4	802.11b	BR	1	15	HIGH	Efficiency based
6	1	6	802.11b	BR	1	15	HIGH	Efficiency based
7	1	8	802.11b	BR	1	15	HIGH	Efficiency based
8	1	10	802.11b	BR	1	15	HIGH	Efficiency based
9	1	12	802.11b	BR	1	15	HIGH	Efficiency based
10	3	-15	802.11b	BR	1	20	MEDIUM	Efficiency based
11	3	-5	802.11b	BR	1	20	MEDIUM	Efficiency based
12	3	0	802.11b	BR	1	20	MEDIUM	Efficiency based
13	3	4	802.11b	BR	1	20	MEDIUM	Efficiency based
14	3	6	802.11b	BR	1	20	MEDIUM	Efficiency based
15	3	8	802.11b	BR	1	20	MEDIUM	Efficiency based
16	3	10	802.11b	BR	1	20	MEDIUM	Efficiency based
17	3	12	802.11b	BR	1	20	MEDIUM	Efficiency based
18	5	-15	802.11n	BR	1	35	LOW	IMD3_Optimized
19	5	-5	802.11n	BR	1	35	LOW	IMD3_Optimized
20	5	0	802.11n	BR	1	35	LOW	IMD3_Optimized
21	5	4	802.11n	BR	1	35	LOW	IMD3_Optimized
22	5	6	802.11n	BR	1	35	LOW	IMD3_Optimized
23	5	8	802.11n	BR	1	35	LOW	IMD3_Optimized
24	5	10	802.11n	BR	1	35	LOW	IMD3_Optimized
25	5	12	802.11n	BR	1	35	LOW	IMD3_Optimized

Figure 5.6: Organized WLAN Victim Data for Measurement Parameters and Power Bins

Based on this sorted data, the arbitration decisions for WLAN and Bluetooth are made independently and stored with respect to their corresponding parameter sets. A logical AND operation is performed on the values of both by accurately matching the parameter sets, isolation levels, and transmit power combinations. Figure 5.7 below shows a portion of the final TX Arbitration sheet, which is generated as the output of the third stage.

	A	B	C	D	E	F	G	H	I	J	K	L	M	N	O	P	Q
1			802.11b/ HIGH/ Efficiency based/ BR					802.11b/ MEDIUM/ IMD3_Optimized/ BR					802.11n/ LOW / Efficiency based / EDR				
2		Isolation	15	20	25	30	35	15	20	25	30	35	15	20	25	30	35
3	WL_Tx	BT_Tx															
4	1	-15	1	1	1	1	1	1	1	1	1	1	1	1	1	1	1
5		-5	1	1	1	1	1	1	1	1	1	1	1	1	1	1	1
6		0	1	1	1	1	1	1	1	1	1	1	1	1	1	1	1
7		4	1	1	1	1	1	1	1	1	1	1	1	1	1	1	1
8		6	1	1	1	1	1	1	1	1	1	1	1	1	1	1	1
9		8	1	1	1	1	1	1	1	1	1	1	1	1	1	1	1
10		10	1	1	1	1	1	1	1	1	1	1	1	1	1	1	1
11		12	1	1	1	1	1	1	1	1	1	1	1	1	1	1	1
12	3	-15	0	1	1	1	1	1	1	1	1	1	1	1	1	1	1
13		-5	1	1	1	1	1	1	1	1	1	1	1	1	1	1	1
14		0	1	1	1	1	1	1	1	1	1	1	1	1	1	1	1
15		4	1	1	1	1	1	1	1	1	1	1	1	1	1	1	1
16		6	0	1	1	1	1	1	1	1	1	1	0	1	1	1	1
17		8	0	1	1	1	1	0	1	1	1	1	0	1	1	1	1
18		10	0	0	1	1	1	0	1	1	1	1	0	0	1	1	1
19		12	0	0	1	1	1	0	0	1	1	1	0	0	1	1	1

Figure 5.7: Final TX Arbitration Sheet

5.1.4 Stage 4: Output After Applying Power Backoff Technique

The output of this stage consists of the feedback powers evaluated for both WLAN and Bluetooth when each is considered the lower-priority radio. Two separate Excel sheets are generated, one for each scenario. Figure 5.8 and 5.9 displays a sample of the WLAN and Bluetooth feedback powers corresponding to selected test parameter combinations, as obtained after the execution of the fourth stage of the algorithm.

	A	B	C	D	E	F	G	H	I	J
1						Antenna Isolation				
2	Frequency Separation	BT_DataRate	WLAN_ modulation	Power Table Type	WLAN power (dBm)	15	20	25	30	35
3	HIGH	BR	802.11b	Efficiency based	1	12	12	12	12	12
4	HIGH	BR	802.11b	Efficiency based	5	4	8	12	12	12
5	HIGH	BR	802.11b	Efficiency based	9	-5	0	6	10	12
6	MEDIUM	BR	802.11b	IMD3_Optimized	1	12	12	12	12	12
7	MEDIUM	BR	802.11b	IMD3_Optimized	5	6	10	12	12	12
8	MEDIUM	BR	802.11b	IMD3_Optimized	9	-5	4	8	12	12
9	LOW	EDR	802.11n	Efficiency based	1	12	12	12	12	12
10	LOW	EDR	802.11n	Efficiency based	5	4	8	12	12	12
11	LOW	EDR	802.11n	Efficiency based	9	-5	0	6	10	12

Figure 5.8: Feedback Powers - WLAN Low Priority Scenario

	A	B	C	D	E	F	G	H	I	J
1						Antenna Isolation				
2	Frequency Separation	BT_DataRate	WLAN_ modulation	Power Table Type	BT power (dBm)	15	20	25	30	35
3	HIGH	BR	802.11b	Efficiency based	-15	1	5	10	15	17
4	HIGH	BR	802.11b	Efficiency based	-5	5	13	17	17	17
5	HIGH	BR	802.11b	Efficiency based	0	5	10	15	17	17
6	MEDIUM	BR	802.11b	IMD3_Optimized	-15	5	5	15	17	17
7	MEDIUM	BR	802.11b	IMD3_Optimized	-5	13	17	17	17	17
8	MEDIUM	BR	802.11b	IMD3_Optimized	0	10	13	17	17	17
9	LOW	EDR	802.11n	Efficiency based	-15	3	5	13	17	17
10	LOW	EDR	802.11n	Efficiency based	-5	5	15	17	17	17
11	LOW	EDR	802.11n	Efficiency based	0	5	10	17	17	17

Figure 5.9: Feedback Powers - Bluetooth Low Priority Scenario

5.1.5 Stage 5 & 6: Output of Prepared Register Configurations

The register values are computed and stored in a final text file, which serves as the complete output of the automation process. The results from Stage 5 consist of the evaluated register settings, while Figure 5.10 and 5.11 illustrates the final output from Stage 6, which incorporates these values along with the complete set of results obtained in the previous stage.

```
TX_arb_registers; Isolation: 15 dB

    {0X001, 0x027FFF9D},
    {0X002, 0x00000002},
    {0X003, 0x0EFF0FAA},
    {0X004, 0x0003A002},
    {0X005, 0x027FEFFF},
    {0X006, 0x0000CD62},
    {0X007, 0x0EFF8FFF},

TX_arb_registers; Isolation: 20 dB

    {0X001, 0x0375FF9D},
    {0X002, 0x0000004D},
    {0X003, 0x9A1F0FAA},
    {0X004, 0x0074C002},
    {0X005, 0x027FEA3F},
    {0X006, 0x0001DC61},
    {0X007, 0x0EFF8FEF},
```

Figure 5.10: Final Automation Output 1 - TX Arbitration Hardware Register Addresses and Respective Values

```
Feedback_pwr_registers; Isolation: 15 dB

    {0X010, 0x0375FF9D},
    {0X011, 0x0000004D},
    {0X012, 0x9A1F0FAA},
    {0X013, 0x0074C002},
    {0X014, 0x027FEA3F},
    {0X015, 0x0001DC61},
    {0X016, 0x0EFF8FEF},

Feedback_pwr_registers; Isolation: 20 dB

    {0X010, 0x00000F9D},
    {0X011, 0x0001ACC0},
    {0X012, 0x9A100000},
    {0X013, 0x0000A200},
    {0X014, 0x000014CD},
    {0X015, 0x00010AC4},
    {0X016, 0x001FFEA0},
```

Figure 5.11: Final Automation Output 2 - Hardware Register Addresses and Respective Values Representing Power Backoff Technique

These images display sample register addresses along with their corresponding values. A more extensive set of register configurations is similarly generated using the tool.

5.2 Conclusion

This thesis presented a detailed investigation into the interferences caused by the third-order intermodulation distortion (IMD3) in multi-radio wireless systems. The major focus was on Bluetooth and WLAN coexistence scenarios. The increasing demand for high-throughput and energy-efficient communication in integrated systems makes IMD3 a critical factor that can impact overall performance and compliance with regulatory standards.

To address this issue, two effective mitigation strategies, TX Arbitration and Power Backoff, were explored and implemented. These techniques were developed and executed through a robust Python-based automation tool designed to handle large-scale IMD3 measurement data. The framework was built in sequential stages, enabling the tool to effectively make TX arbitration decisions and determine feedback powers for both radios.

Throughout this work, careful attention was paid to preserving data integrity and aligning software logic with hardware constraints. The developed solution not only provides a practical approach to mitigate IMD3 but also serves as a scalable framework that can be extended to other coexistence scenarios or newer radio standards.

In conclusion, the thesis successfully demonstrates how a systematic, data-driven approach can be leveraged to manage complex interference issues in modern wireless systems. The results highlight the effectiveness of combining analytical methods with automation to streamline IMD3 mitigation and ensure regulatory compliance.

5.3 Future Scope

The future scope of this work includes the integration of adaptive machine learning algorithms to enable real-time prediction and dynamic optimization of IMD3 performance.

Enhancements to the automation tool could involve expanding support for additional radio technologies and more complex coexistence scenarios involving multiple simultaneous radios. Further research may focus on hardware-in-the-loop validation to verify the software-generated arbitration and power backoff decisions on physical chipsets, thereby improving the accuracy and reliability of the proposed methods. Moreover, incorporating this framework within a broader system-level power management and interference mitigation strategy could provide a more comprehensive approach to addressing coexistence challenges in multi-radio environments.

REFERENCES

[1] S. He, B. Zhang, J. Luo, and M. Qu, “Research on coexistence and mutual interference of Wi-Fi and Bluetooth,” *2021 Int. Conf. Microw. Millim. Wave Technol. ICMMT 2021 - Proc.*, 2021, doi: 10.1109/ICMMT52847.2021.9617988.

[2] Y. K. Kwok and M. C. H. Chek, “Design and evaluation of coexistence mechanisms for bluetooth and IEEE 802.11b systems,” *IEEE Int. Symp. Pers. Indoor Mob. Radio Commun. PIMRC*, vol. 3, pp. 1767–1771, 2004, doi: 10.1109/PIMRC.2004.1368303.

[3] K. Pahlavan and P. Krishnamurthy, “Evolution and Impact of Wi-Fi Technology and Applications: A Historical Perspective,” *Int. J. Wirel. Inf. Networks*, vol. 28, no. 1, pp. 3–19, Mar. 2021, doi: 10.1007/S10776-020-00501-8/FIGURES/7.

[4] C. Bisdikian, “An overview of the Bluetooth wireless technology,” *IEEE Commun. Mag.*, vol. 39, no. 12, pp. 86–94, Dec. 2001, doi: 10.1109/35.968817.

[5] C. D. M. Cordeiro, S. Abhyankar, R. Toshiwal, and D. P. Agrawal, “A novel architecture and coexistence method to provide global access to/from bluetooth WPANs by IEEE 802.11 WLANs,” *IEEE Int. Performance, Comput. Commun. Conf. Proc.*, pp. 23–30, 2003, doi: 10.1109/PCCC.2003.1203680.

[6] C. F. Chiasserini and R. R. Rao, “Coexistence mechanisms for interference mitigation in the 2.4-GHz ISM band,” *IEEE Trans. Wirel. Commun.*, vol. 2, no. 5, pp. 964–975, Sep. 2003, doi: 10.1109/TWC.2003.817417.

[7] R. G. Garroppo, L. Gazzarrini, S. Giordano, and L. Tavanti, “Experimental assessment of the coexistence of Wi-Fi, ZigBee, and bluetooth devices,” *2011 IEEE Int. Symp. a World Wireless, Mob. Multimed. Networks, WoWMoM 2011 - Digit. Proc.*, 2011, doi: 10.1109/WOWMOM.2011.5986182.

[8] C. F. Chiasserini and R. R. Rao, “Coexistence mechanisms for interference mitigation between IEEE 802.11 WLANs and Bluetooth,” *Proc. - IEEE INFOCOM*, vol. 2, pp.

590–598, 2002, doi: 10.1109/INFCOM.2002.1019304.

[9] K. Matheus and S. Zürbes, “Co-existence of bluetooth and IEEE 802.11B WLANS: Results from a radio network testbed,” *IEEE Int. Symp. Pers. Indoor Mob. Radio Commun. PIMRC*, vol. 1, pp. 151–155, 2002, doi: 10.1109/PIMRC.2002.1046679.

[10] G. R. Hiertz, D. Denteneer, L. Stibor, Y. Zang, X. P. Costa, and B. Walke, “The IEEE 802.11 universe,” *IEEE Commun. Mag.*, vol. 48, no. 1, pp. 62–70, Jan. 2010, doi: 10.1109/MCOM.2010.5394032.

[11] “Bluetooth Technology Overview | Bluetooth® Technology Website.” https://www.bluetooth.com/learn-about-bluetooth/tech-overview/ (accessed Sep. 02, 2024).

[12] R. Shorey and B. A. Miller, “Bluetooth technology: merits and limitations,” *IEEE Int. Conf. Pers. Wirel. Commun.*, pp. 80–84, 2000, doi: 10.1109/ICPWC.2000.905777.

[13] R. Challoo, A. Oladeinde, N. Yilmazer, S. Ozcelik, and L. Challoo, “An Overview and Assessment of Wireless Technologies and Co- existence of ZigBee, Bluetooth and Wi-Fi Devices,” *Procedia Comput. Sci.*, vol. 12, pp. 386–391, Jan. 2012, doi: 10.1016/J.PROCS.2012.09.091.

[14] L. Ophir, Y. Bitran, and I. Sherman, “WI-FI (IEEE802.11) and bluetooth coexistence: Issues and solutions,” *IEEE Int. Symp. Pers. Indoor Mob. Radio Commun. PIMRC*, vol. 2, pp. 847–852, 2004, doi: 10.1109/PIMRC.2004.1373819.

[15] B. Razavi and R. Behzad, *RF microelectronics*. 2012.

[16] S. W. Tam *et al.*, “A 28 nm CMOS Dual-Band Concurrent WLAN and Narrow Band Transmitter With On-Chip Feedforward TX-to-TX Interference Cancellation Path for Low Antenna-to-Antenna Isolation in IoT Devices,” *IEEE J. Solid-State Circuits*, vol. 59, no. 5, pp. 1301–1311, May 2024, doi: 10.1109/JSSC.2024.3352532.

[17] N. Males-Ilic, B. Milovanovic, and D. Budimir, “Low intermodulation amplifiers for RF and microwave wireless systems,” *Asia-Pacific Microw. Conf. Proceedings, APMC*, vol. 3, pp. 984–987, 2001, doi: 10.1109/APMC.2001.985282.

[18] Z. Jing, A. Waltho, Y. Xue, and G. Xingang, “Multi-radio coexistence: Challenges and opportunities,” *Proc. - Int. Conf. Comput. Commun. Networks, ICCCN*, pp. 358–364, 2007, doi: 10.1109/ICCCN.2007.4317845.

[19] H. Garlan, “FCC Improves Spectrum Utilization Thru Use of Part 15,” pp. 1–4, Sep. 2016, doi: 10.1109/ISEMC.1973.7569828.

[20] B. Zhen, Y. Kim, and K. Jang, “The analysis of coexistence mechanisms of Bluetooth,” *IEEE Veh. Technol. Conf.*, vol. 1, pp. 419–423, 2002, doi: 10.1109/VTC.2002.1002748.

[21] A. Hasan and B. M. Khan, “Coexistence Management in Wireless Networks-A Survey,” *IEEE Access*, vol. 10, pp. 38600–38624, 2022, doi: 10.1109/ACCESS.2022.3165223.

[22] “US11716101B2 - Multi-radio device - Google Patents.” https://patents.google.com/patent/US11716101B2/ (accessed Jun. 01, 2025).